

High-energy cosmic-ray nuclei from high- and low-luminosity gamma-ray bursts and implications for multi-messenger astronomy

Kohta Murase^{1,*}, Kunihiro Ioka², Shigehiro Nagataki¹, and Takashi Nakamura³

¹*Yukawa Institute for Theoretical Physics, Kyoto University,
Oiwake-cho, Kitashirakawa, Sakyo-ku, Kyoto, 606-8502, Japan*

²*Theory Division, KEK (High Energy Accelerator Research Organization), 1-1 Oho, Tsukuba 305-0801, Japan*

³*Department of Physics, Kyoto University, Kyoto 606-8502, Japan*

(Dated: June 21, 2024)

Gamma-ray burst (GRB) is one of the candidates of high-energy cosmic-ray acceleration sites. They may be also ultra-high-energy ($\gtrsim 10^{18.5}$ eV) cosmic-ray (UHECR) sources. In this paper, we discuss possibilities and implications of high-energy cosmic-ray acceleration in GRBs. (i) First, we show that not only protons but also heavier nuclei can be accelerated up to ultra-high energies in both usual high-luminosity (HL) and low-luminosity (LL) GRBs by using the Geant4. LL GRBs may also make a significant contribution to the observed UHECR flux if they form a distinct population, and we investigate cosmic-ray acceleration in LL GRBs in detail. (ii) Second, we discuss implications of the GRB-UHECR hypothesis (and Hypervnova-UHECR hypothesis) to cosmic-ray astronomy. HL GRBs and LL GRBs will lead to different source number densities as UHECR sources, so that the determination of the number density of UHECR sources and strength of the mean extragalactic magnetic field (EGMF) will give us useful clues to test the hypothesis. If the EGMF is sufficiently weak, only LL GRBs can be dominant as UHECR sources. If the EGMF is sufficiently strong, HL GRBs would be more suitable UHECR sources to explain the observed anisotropy. (iii) The detection of high-energy neutrinos and gamma rays will also give us important clues to high-energy cosmic-ray acceleration in GRBs. We show that, when ultra-high-energy heavy nuclei such as iron can survive in GRBs, the detection of high-energy neutrinos would become more difficult. However, since escape of high-energy gamma rays from the source is easier in such cases, the detection of very high-energy gamma rays and/or secondary delayed gamma rays can be more expected.

PACS numbers: 95.85.Ry, 98.70.Rz, 25.20.-x, 14.60.Lm, 96.50.Pw, 98.70.Sa

I. INTRODUCTION

Gamma-ray bursts (GRBs) and supernovae (SNe) are the most powerful phenomena in the universe. The latter is believed to be the origin of high-energy cosmic rays below the knee $\approx 10^{15.7}$ eV. The former could also accelerate baryons up to high energies if the dissipation process is due to shock dissipation. Waxman, Milgrom & Usov and Vietri suggested that ultra-high-energy cosmic rays (UHECRs) are produced in GRBs [1, 2, 3]. Their suggestions were based on the two arguments. First is the requirement that relativistic outflows that make GRBs satisfy various conditions for baryons to be accelerated up to greater than 10^{20} eV. Second is that the energy generation rate required to account for the observed UHECR flux is comparable to the energy generation rate of observed gamma rays. The latter argument depends on the local GRB rate which is not well known observationally. Recent *Swift* observations have suggested that the cosmological high-luminosity GRB (HL GRB) rate increases rapidly with the redshift z , and the local GRB rate may be somewhat smaller compared to some estimations in the pre-*Swift* era (see, e.g., [4, 5, 6]). If the local GRB rate is not high enough, the required baryon loading becomes larger [7, 8, 9]. In addition, if the UHECR spectrum at

the source is steeper than that with the spectral index $p \sim 2$ (as expected in the dip model [9, 10]), the total nonthermal cosmic-ray energy of GRBs, necessary for explaining the observed UHECR flux, would be larger than the radiation energy. Despite such caveats, the GRB-UHECR hypothesis is still one of the most interesting possibilities for explanation of observed UHECRs, and it should be examined by future observations.

Recent observations have tentatively suggested that some GRBs may form a different class (see, e.g., [11, 12]). Some long-duration GRBs like GRB 980425 and GRB 060218 are associated with core-collapse supernovae (SNe of TypeIc to be more specific). As Guetta et al. [13] argued, no bright bursts at $z < 0.17$ should have been observed by a HETE-like instruments within the 20 years, if the logN-logP relationship of HL GRBs continues to the low-luminosity region. Therefore, the unexpected discovery of low-luminosity GRB 060218 lead to the idea that they form a different new class of GRBs from the conventional HL GRBs, and GRBs in this class are called low-luminosity GRBs (LL GRBs) or sub-energetic GRBs, which may be more common than HL GRBs. If this speculation is true, they can provide the significant energy as high-energy cosmic rays, neutrinos and gamma rays. Murase et al. [14] suggested that cosmic rays can be accelerated up to ultra-high energies ($\gtrsim 10^{18.5}$ eV) in LL GRBs, and LL GRBs may make an important contribution to the observed high-energy cosmic-ray flux and the diffuse neutrino background [14, 15]. Such LL GRBs

*Electronic address: kmurase@yukawa.kyoto-u.ac.jp

were associated with energetic supernovae called hypernovae. As in cases of supernovae, cosmic-ray acceleration is expected at shocks formed by the high-velocity ejecta. In fact, if the magnetic field is sufficiently amplified, cosmic-rays can be accelerated up to very high energies, even to ultra-high energies. Wang et al. [16, 17] suggested that they could explain observed high-energy cosmic rays above the second knee, under the assumption that LL GRBs have the enough local rate higher than that of HL GRBs. Therefore, if high-energy cosmic rays are produced by GRB outflows and/or hypernovae, we can expect that not only usual HL GRBs but also LL GRBs can make an important contribution.

The origin of UHECRs has been one of the biggest mysteries in the universe. In order to reveal the origin of UHECRs, UHECRs observatories with larger exposures have been constructed. Now, the total exposure of (South) Pierre Auger Observatory (PAO) already exceeds past detectors such as Akeno Giant Air Shower Array (AGASA). PAO collects many events, and the UHECR spectrum deduced by PAO suggests the existence of the Greisen-Zatsepin-Kuz'min (GZK) cut-off energy which arises from the photomeson production process between UHECRs and cosmic microwave background (CMB) photons [18, 19]. In addition, PAO recently revealed the anisotropy and rejected the isotropy of UHECRs above 60 EeV at 3σ level [20, 21]. They also suggested that the positional correlation between nearby sources such as Active galactic nuclei (AGN). Although PAO results suggest that the distribution of UHECRs traces the matter distribution in the universe, the origin of UHECRs is still unknown, that is, AGNs, GRBs and other possibilities remain (see the latest review for AGN and GRBs, e.g., [22]).

The preliminary elongation rate data by PAO showed the break around $\sim 10^{18.35}$ eV [23]. Whether heavier nuclei becomes more important above this break as the energy increases (which seems conflict with Hires data) is still under debate. It is because there are large uncertainties in hadronic interactions (where different hadronic models lead to different results). In addition, recent results on UHECRs above 60 EeV by PAO may infer that protons are dominant sources [20, 21], while some authors dispute [24, 25]. Although the issue of the composition of UHECRs requires more and more studies, present data seem to allow the presence of significant fractions of ultra-high-energy (UHE) nuclei around the GZK cut-off energy, even if protons are dominant. Therefore, it is one of the interesting issues whether UHE nuclei can survive (i.e., UHE nuclei are not photodisintegrated and not depleted due to photomeson production during the dynamical time) or not.

In this paper, we study production of high-energy cosmic-ray nuclei in GRBs. Especially, we show that UHECRs can be produced in both of HL GRB and LL GRBs, where we evaluate various time scales by using numerical calculations. Then, we show that both of HL GRBs and LL GRBs can supply the required amount

of UHECRs, if their nonthermal cosmic-ray energy in the UHECR energy range is comparable to their radiation energy. We also discuss various implications of the GRB-UHECR hypothesis (including the HLGRB-UHECR, LLGRB-UHECR and Hypernova-UHECR hypotheses) to cosmic-ray astronomy. We see that the determination of the number density of UHECR sources and extragalactic magnetic field (EGMF) strength is essential to test the hypothesis.

Not only cosmic-ray astronomy but also neutrino and gamma-ray astronomy are also important. High-energy neutrinos can be produced because sufficiently high-energy protons can produce pions and kaons via the photomeson production process and/or pp reaction. Now, large neutrino detectors such as IceCube [26], KM3Net [27] are being constructed. ANITA [28] and PAO [29] can also detect very high-energy neutrinos. We have chances to see such high-energy neutrino signals in the future.

High-energy neutrino signals from HL GRBs were predicted in the context of the standard scenario of GRBs assuming that observed UHECRs come from GRBs [30, 31, 32, 33]. Murase & Nagataki [8] also investigated the neutrino emission from HL GRBs in detail. High-energy neutrinos from flares in the early afterglow phase are also expected [34]. Various predictions in the early afterglow phase are carefully studied and summarized in Ref. [35]. High-energy neutrino signals from GRBs are very useful as a direct probe of cosmic-ray acceleration in GRBs.

We can expect high-energy gamma rays as well as high-energy neutrinos. However, in some cases, very high-energy gamma rays cannot escape from the GRB source due to internal attenuation (see e.g., [36, 37] and references there in). However, when UHE heavy nuclei can survive, we expect that the photon density is small. In fact, we can show that very high-energy gamma rays can escape from the source under conditions where UHE heavy nuclei can survive. Very high-energy gamma-ray emission is also expected in the hypernova model. We can detect these high-energy gamma-ray signals if the source is nearby. If the source is far away, high-energy gamma rays above \sim TeV are attenuated by the cosmic microwave/infrared background (CMB/CIB) photons, and cascaded gamma rays are generated. Secondary gamma rays may be observed by upcoming Gamma-Ray Large Area Telescope (GLAST) and Cherenkov telescopes (see e.g., [38] and references there in).

The structure of this paper is as follows. In Sec. II, we show that cosmic rays (protons and heavier nuclei) can be accelerated up to ultra-high energies in GRBs. We consider the internal, reverse and external shock models. In Sec. III, we briefly review the energetics of GRBs and UHECRs. In Sec. IV, we discuss various implications of the GRB-UHECR hypothesis to cosmic-ray astronomy. In Sec. V and Sec. VI, we also describe implications to neutrino and gamma-ray astronomy. Especially, we show that, when UHE nuclei survive in GRBs, the detection of high-energy neutrinos would be more difficult while

the detection of very high-energy gamma rays can be expected. Hereafter, we shall use notations such as $Q_x = Q/10^x$ in cgs units.

II. ACCELERATION OF COSMIC-RAY NUCLEI IN GRBS

In the standard model of GRBs (for reviews, see, e.g., [39, 40, 41]), both of the prompt and afterglow emission are attributed to electromagnetic radiation from relativistic electrons accelerated in shocks. If relativistic outflows that make GRBs contain baryons, not only electrons but also protons (and heavier nuclei) will be accelerated. Although the detail of the acceleration mechanism is poorly known, we usually assume that the first-order Fermi acceleration mechanism works in GRBs, where the distribution of nonthermal cosmic rays is given by a power-law spectrum under the test-particle approximation (see reviews, e.g., [42]). Therefore, the cosmic-ray spectrum can be written as [35, 43]

$$\frac{dn_{\text{CR}}}{d\varepsilon_{\text{CR}}} = \frac{U_{\text{CR}}}{\int_{\varepsilon_{\text{CR}}^{\min}}^{\varepsilon_{\text{CR}}^{\max}} d\varepsilon_{\text{CR}} \varepsilon_{\text{CR}}^{-(p-1)}} \varepsilon_{\text{CR}}^{-p}, \quad (1)$$

where ε_{CR} is the energy of cosmic rays in the comoving frame, U_{CR} is the comoving cosmic-ray energy density, and p is the spectral index. For non-relativistic shocks, we can obtain $p = 2$ for the compression ratio $r_c = 4$ in the test-particle approximation. As the shock-speed increases, the spectral index can deviate from values for non-relativistic shocks. In the diffusive small pitch-angle scattering regime, $p \simeq 2.2$ is obtained in the ultra-relativistic limit [44]. But the large-angle scattering can lead to harder spectral indices [45, 46]. As a shock becomes relativistic, the particle-energy gain becomes larger, which lead to shortening of the acceleration time scale [49]. The acceleration time scale is written as [47, 48, 49]

$$t_{\text{acc}} = \eta \frac{\varepsilon_N}{ZeBc}. \quad (2)$$

Here, ε_N is the cosmic-ray energy in the comoving frame and η is a pre-factor. For the most efficient acceleration, we expect $\eta \sim (1-10)$ [47]. Throughout this paper $\eta = 1$ is used. Note that Eq. (2) could be used for the second-order Fermi acceleration mechanism when the Alfvén-wave speed is close to the light speed. The maximum energy of cosmic-rays is determined by several criteria. One is derived from the requirement that the Larmor radius of a particle should be smaller than the effective size of the acceleration region (the Hillas condition). In addition, the acceleration time scale should be smaller than the dynamical time scale t_{dyn} (which is essentially the same as the Hillas condition in our interested cases) and escape time scale t_{esc} . The maximum energy is also limited by the total cooling time scale $t_{\text{cool}}^{-1} \equiv t_{N\gamma}^{-1} + t_{\text{syn}}^{-1} + t_{\text{IC}}^{-1} + t_{\text{ad}}^{-1}$. Here, t_{syn} is the synchrotron cooling time scale, t_{IC} is

the inverse-Compton cooling time scale and t_{ad} is the adiabatic cooling time scale. In cases of GRBs, we shall use $t_{\text{ad}} \approx t_{\text{dyn}}$ [30, 35, 50]. (Actually, the adiabatic loss and escape of cosmic rays should be taken into account carefully, because the cosmic-ray spectrum could be modified by these effects. Unfortunately, quantitative estimation is difficult and it is beyond the scope of this paper.) For descriptions of various time scales, see, e.g., Refs. [35, 47, 50] and references there in. $t_{N\gamma}$ is the photohadronic cooling time scale which includes the photodisintegration, photomeson production and photopair production processes. For protons with sufficiently high energies, the photomeson production process is the most important, whose time scale is given by

$$t_{p\gamma}^{-1}(\varepsilon_p) = \frac{c}{2\gamma_p^2} \int_{\bar{\varepsilon}_{\text{th}}}^{\infty} d\bar{\varepsilon} \sigma_{p\gamma}(\bar{\varepsilon}) \kappa_p(\bar{\varepsilon}) \bar{\varepsilon} \int_{\bar{\varepsilon}/2\gamma_p}^{\infty} d\varepsilon \varepsilon^{-2} \frac{dn}{d\varepsilon}, \quad (3)$$

where $\bar{\varepsilon}$ is the photon energy in the rest frame of proton, γ_p is the proton's Lorentz factor, κ_p is the inelasticity of proton, and $\bar{\varepsilon}_{\text{th}} \approx 145$ MeV is the threshold photon energy for photomeson production. For heavy nuclei, the photodisintegration and photomeson production processes are important, whose time scale is given by

$$t_{N\gamma}^{-1}(\varepsilon_N) = \frac{c}{2\gamma_N^2} \int_{\bar{\varepsilon}_{\text{th}}}^{\infty} d\bar{\varepsilon} \sigma_{N\gamma}(\bar{\varepsilon}) \bar{\varepsilon} \int_{\bar{\varepsilon}/2\gamma_N}^{\infty} d\varepsilon \varepsilon^{-2} \frac{dn}{d\varepsilon}, \quad (4)$$

where γ_N is the nucleon's Lorentz factor, $\bar{\varepsilon}_{\text{th}}$ is the threshold photon energy for photodisintegration which is given in Ref. [51]. In order to evaluate Eqs. (3) and (4), we use the numerical simulation kit Geant4 [52], which includes the cross section data based on experimental data [53]. As seen later, it is important to use the accurate cross section in the high-energy range. Although we evaluate $t_{N\gamma}$ by numerical calculations, the simple analytic treatment is often useful. The most frequently used approximation for the photomeson production process is the Δ -resonance approximation (see, e.g., [30, 34]). The corresponding one for the photodisintegration process is the Giant-Dipole-Resonance (GDR) approximation. Similarly, we can apply it to the GDR approximation for a broken power-law photon spectrum. We have

$$t_{N\gamma}^{-1} \simeq \frac{U_\gamma}{5\varepsilon^b} c \sigma_{\text{res}} \kappa(\bar{\varepsilon}) \frac{\Delta\bar{\varepsilon}}{\bar{\varepsilon}_{\text{res}}} \begin{cases} (E_N/E_N^b)^{\beta-1} \\ (E_N/E_N^b)^{\alpha-1} \end{cases}, \quad (5)$$

where $E_N^b \simeq 0.5\bar{\varepsilon}_{\text{res}} m_N c^2 \Gamma^2 / \varepsilon_{\text{ob}}^b$, α is a photon index in lower energies while β in higher energies. The parameter regions for the upper and lower columns are $E_N < E_N^b$ and $E_N \geq E_N^b$, respectively. Here $\varepsilon_{\text{ob}}^b$ is the break energy measured by the observer in the local rest frame, and U_γ is the total photon energy density. For example, a Band function which reproduces spectra of the prompt emission, can be approximated by a broken power-law spectrum. Spectra of afterglows are also expressed by several segments of power-law spectra. The cross section at the resonant energy

$\bar{\epsilon}_{\text{res}}$ is expressed as σ_{res} . For GDR of nucleon, we use $\sigma_{\text{GDR}} \sim 1.45 \times 10^{-27} \text{ cm}^2 A$, $\bar{\epsilon}_{\text{GDR}} \sim 42.65 A^{-0.21} \text{ MeV}$ and $\Delta\bar{\epsilon} \sim 8 \text{ MeV}$ [51, 54, 55, 56]. In the case of Δ -resonance of proton, we use $\sigma_{\Delta} \sim 4 \times 10^{-28} \text{ cm}^2$, $\bar{\epsilon}_{\Delta} \sim 0.3 \text{ GeV}$, $\Delta\bar{\epsilon} \sim 0.2 \text{ GeV}$ and $\kappa_p \sim 0.2$ [30, 34]. These approximations reproduce numerical results well except in high energies. In high energies, the effect of non-GDR (including the photomeson production process) can become important, as seen later. This tendency can also be seen in $t_{p\gamma}$. As pointed out in Ref. [8], the effect of non-resonance becomes moderately important in high energies for spectra of the prompt emission where $\alpha \sim 1$.

Next, let us introduce the optical depth for photomeson production. We define $f_{N\gamma} \equiv t_{\text{dyn}}/t_{N\gamma}$. This quantity expresses whether cosmic rays can survive in the source or not. That is, cosmic rays can survive from the photodisintegration and/or photomeson production processes if $f_{N\gamma} < 1$, while not if $f_{N\gamma} \geq 1$.

In the following subsections, we shall show that high-energy cosmic-ray nuclei can be produced in the internal and external shock models for HL and LL GRBs. GRBs may be even UHECR sources. In such cases, note that cosmic rays have to be accelerated above 10^{20} eV from observations of the highest energy events and the existence of the bump around the GZK cutoff energy. We shall allow for possibilities that observed highest UHECRs are UHE nuclei. It is because, although the arrival distribution and spectrum of UHECRs are consistent with the proton model, some authors claimed that UHE nuclei are more important.

A. Internal Shock Model

The internal shock model is one of the most frequently discussed models in order to explain the prompt emission. Relativistic outflows make internal collisions, which lead to internal dissipation via shocks. The formed shocks will be mildly relativistic shocks, and charged particles will be accelerated at those collisionless shocks by some mechanism such as the Fermi acceleration mechanism. HL GRBs have luminosity $L_{\gamma} \sim 10^{51-52} \text{ erg s}$ and the observed peak energy $\epsilon_{\text{ob}}^b \sim 10^{2.5} \text{ keV}$. The isotropic equivalent energy is $E_{\gamma}^{\text{iso}} \sim 10^{53} \text{ ergs}$ $L_{\gamma,52}[\delta t_{-1}/(1+z)]N_2$. Here δt is the variability time which can vary in the very wide range and N is the number of collisions. A typical collision radius will be expressed by commonly used relation, $r \approx 1.2 \times 10^{14} \Gamma_{2.5}^2 [\delta t/0.02(1+z) \text{ s}] \text{ cm}$. Of course, this radius has to be smaller than the deceleration radius where the afterglow begins. As discussed in Refs. [8, 36, 57], an internal collision radius is one of the most important quantities for the photomeson production. A collision radius $r \sim 10^{13-15} \text{ cm}$ is frequently assumed. The magnetic field is given by $B = 7.3 \times 10^4 \text{ G} \epsilon_B^{1/2} (\Gamma_{\text{sh}}(\Gamma_{\text{sh}} - 1)/2)^{1/2} L_{\text{M},52}^{1/2} \Gamma_{2.5}^{-1} r_{14}^{-1}$. Here, L_{M} is the kinetic luminosity of outflows and Γ_{sh} is the relative Lorentz factor between two subshells. The

typical width of subshells in the comoving frame l is typically given by $l = r/\Gamma$.

Next, let us evaluate maximum energies of cosmic rays by using several criteria. First, $t_{\text{acc}} = t_{\text{dyn}} \approx t_{\text{ad}}$ leads to

$$(1+z)E_{N,\text{ad}}^{\text{max}} = \frac{\Gamma Z e B l}{\eta} \simeq 6.9 \times 10^{20} \text{ eV } Z \eta^{-1} \epsilon_B^{1/2} \epsilon_e^{-1/2} \times \left[\frac{\Gamma_{\text{sh}}(\Gamma_{\text{sh}} - 1)}{2} \right]^{1/2} L_{\gamma,51}^{1/2} \Gamma_{2.5}^{-1}. \quad (6)$$

Note that the Hillas condition $r_L = l = r/\Gamma$ is already satisfied. Second, $t_{\text{acc}} = t_{\text{syn}}$ leads to

$$(1+z)E_{N,\text{syn}}^{\text{max}} = \sqrt{\frac{6\pi Z e}{Z^4 \sigma_T B \eta} \frac{\Gamma m_N^2 c^2}{m_e}} \simeq 4.2 \times 10^{20} \text{ eV } A^2 Z^{-3/2} \eta^{-1/2} \epsilon_B^{-1/4} \epsilon_e^{1/4} \times \left[\frac{\Gamma_{\text{sh}}(\Gamma_{\text{sh}} - 1)}{2} \right]^{-1/4} L_{\gamma,51}^{-1/4} \Gamma_{2.5}^{3/2} r_{14}^{1/2}. \quad (7)$$

Therefore, we can expect that cosmic rays can be accelerated up to ultra-high energies in the internal shock model of HL GRBs unless other cooling time scales such as $t_{p\gamma}$ are important.

The inverse Compton cooling time scale can be also calculated. For evaluation of t_{IC} , we need to give a photon spectrum. The photon spectrum for the prompt emission is often approximated by the broken power-law as

$$\frac{dn}{d\epsilon} = \frac{L_b}{4\pi r^2 \Gamma^2 c (\epsilon^b)^2} \begin{cases} (\epsilon/\epsilon^b)^{-\alpha} & (\text{for } \epsilon^{\min} \leq \epsilon < \epsilon^b) \\ (\epsilon/\epsilon^b)^{-\beta} & (\text{for } \epsilon^b \leq \epsilon \leq \epsilon^{\max}) \end{cases} \quad (8)$$

where L_b is the luminosity at the break energy measured by the observer in the local rest frame, ϵ^{\min} is the minimum cutoff due to synchrotron self-absorption and ϵ^{\max} is the maximum cutoff due to pair-creation in the comoving frame. In this paper, we set $\epsilon^{\min} = 1 \text{ eV}$ and $\epsilon^{\max} = 10 \text{ MeV}$. In this paper, we shall use $\alpha = 1$ and $\beta = 2.2$ as photon indices. Although t_{IC} is calculated, we can usually ignore this cooling time scale due to the Klein-Nishina suppression. Hence, $E_{N,\text{IC}}^{\text{max}}$ is usually larger than $E_{N,\text{syn}}^{\text{max}}$.

The effect of the photomeson production process of protons is investigated in detail in Ref. [8]. For details, see Refs. [8, 35] and references there in. At smaller collision radii, $t_{p\gamma}$ can be more important than other cooling time scales such as t_{syn} . UHE protons are not depleted only at sufficiently large radii. The cross section of photodisintegration is larger than that of photomeson production, so that survival of UHE nuclei is more difficult than survival of UHE protons. We evaluate the maximum energy due to photomeson production and/or photodisintegration, $E_{p,p\gamma}^{\text{max}}$ and/or $E_{N,N\gamma}^{\text{max}}$, from $t_{\text{acc}} = t_{N\gamma}$ and/or $t_{\text{acc}} = t_{p\gamma}$, by evaluating Eqs. (3) and/or (4) numerically.

Our numerical results on various time scales in the internal shock model for HL GRBs are shown in Figs. 1 and 2. For calculations, we give the total photon energy density U_γ by $U_\gamma = \int d\varepsilon \varepsilon (\frac{dn}{d\varepsilon})$. The magnetic field is given by $U_B \equiv \xi_B U_\gamma \approx (\epsilon_B/\epsilon_e) U_\gamma$. Fig. 1 shows the result for $r = 10^{14}$ cm and $\Gamma = 10^{2.5}$. Thick lines show numerical results while thin lines show curves when we use resonance approximations. At sufficiently high energies, we can see that effects of the cross section in the non-resonance region become important. For this typical parameter set, we have the effective optical depth for the photomeson process $f_{p\gamma} \sim 0.3$. Hence, the efficient neutrino production occurs in this parameter set, which can lead to the detectable diffuse neutrino background flux [8, 30]. However, we cannot expect survival of UHE nuclei in such cases. Although they can be accelerated up to very high energies, UHE nuclei cannot survive in the sense that $f_{N\gamma} \gtrsim 1$.

Fig. 2 shows the result for $r = 10^{15}$ cm and $\Gamma = 10^3$. In this parameter set, we expect that UHECR nuclei can survive. Protons and oxygens can be accelerated up to $\sim 10^{20}$ eV and $\sim 10^{21}$ eV, respectively. This is just because the photon density becomes small enough at large radii. Note that we have the effective optical depth for the photomeson process $f_{p\gamma} \sim 10^{-3}$, which is a very small value. In this parameter set, although we can expect survival of UHE nuclei, the magnetic field is also expected to be rather weak as long as we use the conventional value $\xi_B = 1$. Here, we have $B \sim 5.8 \times 10^2$ G, which seems to be somewhat insufficient to explain the observed break energy by the optically thin synchrotron model. (Then, we expect $\varepsilon_{\text{ob}}^b \sim 12 \text{ keV } \Gamma_{2.5} (\Gamma_{\text{sh}} - 1)^2 \epsilon_e^2 g^2 f_e^{-2} B_3$, where $g = g(p) = (p - 2)/(p - 1)$ and p is the electron spectral index). But the detailed mechanism of the prompt emission has not been revealed yet [58], so that we do not consider this problem in this paper. In Fig. 2, we also show curves for spectra with the minimum cutoff energy (thick lines) and that without the cutoff (thin lines). Wang et al. [17] suggested that the effect of minimum cutoff energy (due to self-absorption) can increase the maximum energy of heavy nuclei. However, we see that the effect of self-absorption is not so important even at the highest energies due to the effect of the cross section in the non-resonance region.

Next, let us consider LL GRBs such as GRB 060218 and GRB 980425. For example, GRB 060218 has low luminosity $L_\gamma \sim 10^{46-47}$ ergs/s, which is much smaller than that of usual HL-GRBs [59]. The duration time is $T \sim 3000$ s, and the isotropic equivalent energy is $E_\gamma^{\text{iso}} \sim 10^{50}$ ergs. The observed peak energy is $\varepsilon_{\text{ob}}^b \sim 5$ keV, hence this event is classified as a x-ray flash. Various interpretations for GRB 060218 exist. Several authors suggested the shock break-out model [60, 61]. Other authors argued that this event can be explained by the internal-external shock model [62, 63, 64]. In this paper, we adopt the conventional internal shock model following Toma et al. and we shall adopt the Lorentz factor $\Gamma \sim (5 - 10)$, which is suggested in Refs. [63, 64].

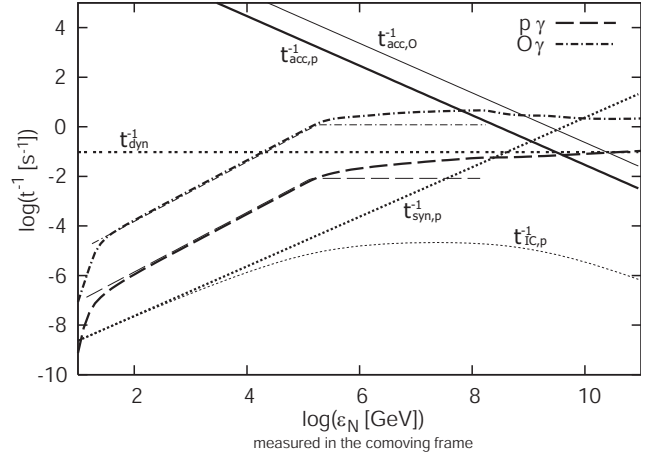


FIG. 1: The acceleration time scale and various cooling time scales of proton and oxygen in the internal shock model for HL GRBs. Energy and time scales are measured in the comoving frame of the outflow. Used parameters are $L_b = 10^{51.5}$ ergs s $^{-1}$, $\varepsilon_{\text{ob}}^b = 10^{2.5}$ keV, $\Gamma = 10^{2.5}$, $r = 10^{14}$ cm and $\xi_B (\approx \epsilon_B/\epsilon_e) = 1$. Thick lines show numerical results on the photomeson and/or photodisintegration time scales. Thin lines show analytic results obtained by the resonance approximation. In the high energies, the effect of the non-resonant cross section becomes important. Note that this parameter set implies that a significant fraction of the energy carried by protons goes into neutrinos.

Collision radii are largely uncertain. In this paper, we adopt $r \sim 10^{14-16}$ cm as fiducial values following Refs. [14, 15, 64]. Collision radii $r \sim 10^{15-16}$ cm imply the time scale $\delta t \sim 10^{2-3}$ s. In fact, the observed light curve of GRB 060218 is somewhat simple and smooth. However, the collision radius may be much smaller as suggested in Ref. [63]. Therefore, we consider these two cases in this paper.

As in cases of HL GRBs, we can evaluate the maximum energies as (see also Ref. [14])

$$(1+z)E_{N,\text{ad}}^{\text{max}} = \frac{\Gamma Z e B l}{\eta} \simeq 2.2 \times 10^{20} \text{ eV } Z \eta^{-1} \epsilon_B^{1/2} \epsilon_e^{-1/2} \times \left[\frac{\Gamma_{\text{sh}}(\Gamma_{\text{sh}} - 1)}{2} \right]^{1/2} L_{\gamma,47}^{1/2} \Gamma_1^{-1} \quad (9)$$

and

$$(1+z)E_{N,\text{syn}}^{\text{max}} = \sqrt{\frac{6\pi Z e}{Z^4 \sigma_T B \eta} \frac{\Gamma m_N^2 c^2}{m_e}} \simeq 7.4 \times 10^{19} \text{ eV } A^2 Z^{-3/2} \eta^{-1/2} \epsilon_B^{-1/4} \epsilon_e^{1/4} \times \left[\frac{\Gamma_{\text{sh}}(\Gamma_{\text{sh}} - 1)}{2} \right]^{-1/4} L_{\gamma,47}^{-1/4} \Gamma_1^{3/2} r_{15}^{1/2}. \quad (10)$$

Therefore, we expect that LL GRBs also can produce UHECRs, especially that UHE nuclei can be accelerated above 10^{20} eV. These two conditions (Eqs. (9) and (10))

equivalently lead to inequalities (ignoring the term $(1+z)$) as

$$\begin{aligned} 0.5Z^{-1}\eta\Gamma_1 E_{N,20} &\lesssim L_{M,48}^{1/2}\epsilon_{B,-1}^{1/2}\left(\frac{\Gamma_{sh}(\Gamma_{sh}-1)}{2}\right)^{1/2} \\ &\lesssim 0.55A^4Z^{-3}\eta^{-1}r_{15}^3\Gamma_1^3E_{N,20}^{-2}, \end{aligned} \quad (11)$$

which is the same as Eq. (2) of Ref. [14]. As seen from the above inequalities, acceleration of protons above $\sim 10^{20}$ eV in LL GRBs will be more difficult than that in HL GRBs, because necessary parameters should be suitably chosen. For protons to be accelerated above $\sim 10^{20}$ eV, relatively more luminous/magnetized LL-GRBs with higher Lorentz factors are required. In fact, GRB 031203, whose redshift and luminosity are intermediate between two dim events (GRB 060218 and GRB 980425) and usual HL GRBs, might be such an event [11, 65]. Eqs. (9) and (10) just mean that UHECR production is also possible in relatively lower luminous GRBs such as XRFs and LL GRBs, even if LL GRBs do not form a distinct population.

Our numerical results are shown in Figs. 3-5. Fig. 3 shows the result for $r = 6 \times 10^{15}$ cm corresponding to $\delta t \sim 1000$ s when we use $r \approx 2\Gamma^2 c \delta t$. We also set $\Gamma = 10$. In this parameter set, we can expect that not only UHECRs can be produced but also accelerated UHE nuclei can survive. This is just because the photon density is small enough at large radii. Note that we have the effective optical depth for the photomeson process $f_{p\gamma} \sim 2 \times 10^{-3}$, which is a small value. In this parameter set, although we can expect survival of UHE nuclei, the magnetic field

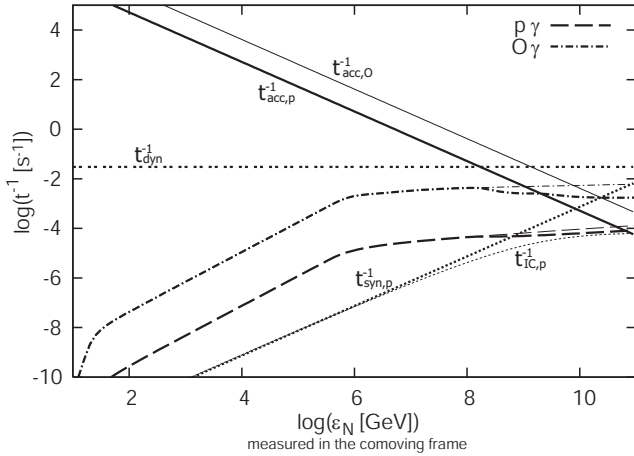


FIG. 2: The same as Fig. 1. But used parameters are $L_b = 10^{51}$ ergs s^{-1} , $\epsilon_{ob}^b = 10^{2.5}$ keV, $\Gamma = 10^3$, $r = 10^{15}$ cm and $\xi_B (\approx \epsilon_B/\epsilon_e) = 1$. Thick lines show numerical results with the synchrotron self-absorption cutoff 1 eV (in the comoving frame). Thin lines show analytic results without the low-energy cutoff for comparison. We can see that the effect of self-absorption is not so important for the maximum energy due to the effect of the non-resonant cross section in the high energies. Note that this parameter set allows for survival of UHE nuclei.

seems to be somewhat weak when we use the conventional value $\xi_B = 1$. In Fig. 3, Fe nuclei can be accelerated up to $\sim 10^{21}$ eV, while protons only up to $\sim 10^{19.5}$ eV.

For comparison, we show the results for the parameter set used in Ref. [14]. In this case, we cannot expect survival of UHE nuclei. Protons can be accelerated up to $\sim 5 \times 10^{19}$ eV while Fe nuclei up to $\sim 10^{20}$ eV (but photodisintegrated). We can also expect the detectable diffuse neutrino background flux as demonstrated in Ref. [14].

In Fig. 5, we show the results for parameters inferred by Ghisellini et al. [63]. A collision radius is small enough, $r = 7 \times 10^{12}$ cm, so that the photomeson production and photodisintegration efficiencies are rather high. Because the photodisintegration and photomeson production processes prohibit acceleration of cosmic rays up to very high-energy, we cannot expect UHECR production in this case.

As noted before, one of the important parameters is a collision radius. Hence, we show maximum energies of proton and heavy nuclei E_N^{\max} as a function of a collision radius r in Fig. 6. In the same figure, $f_{p\gamma}$ and $f_{N\gamma}$ are shown. We can see that the maximum energy of proton is determined by the photomeson production at sufficiently small radii, but usually determined by the synchrotron cooling and adiabatic cooling processes at large radii ($r \gtrsim 10^{12.5}$ cm). The maximum energy of nucleon is usually determined by the photodisintegration and adiabatic cooling. Survival of UHE nuclei is possible only at $r \gtrsim 10^{15}$ cm in this parameter set.

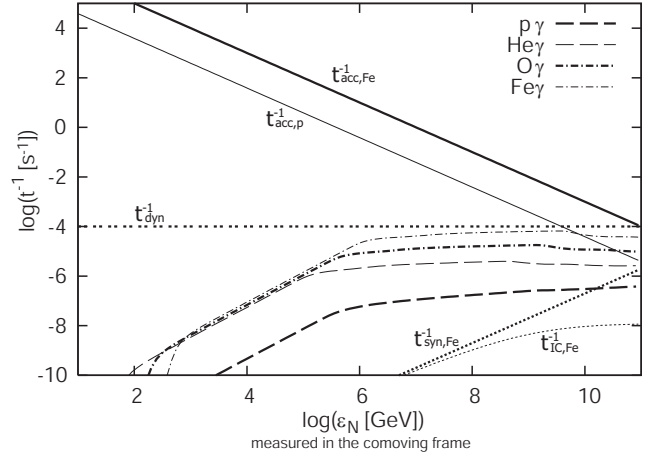


FIG. 3: The acceleration time scale and various cooling time scales of proton, helium, oxygen and iron in the internal shock model for LL GRBs. Energy and time scales are measured in the comoving frame of the outflow. Used parameters are $L_b = 1.5 \times 10^{46}$ ergs s^{-1} , $\epsilon_{ob}^b = 5$ keV, $\Gamma = 10$, $r = 6 \times 10^{15}$ cm (corresponding to $T = 10^3$ s) and $\xi_B (\approx \epsilon_B/\epsilon_e) = 1$. Note that this parameter set allows for survival of UHE nuclei.

B. Reverse Shock Model

The expanding fireball strikes the surrounding medium and will form a reverse shock and forward shock. The shocked ambient and ejecta materials are in pressure balance and are separated by a contact discontinuity. In the original standard model, the reverse shock is thought to be short-lived, which exists during the initial deceleration of the fireball. During this phase, optical/infrared flashes were expected. Indeed, some optical flashes can be interpreted as the reverse shock emission. However, recent observations have reported the tentative lack of bright optical/infrared flashes [66]. Although it is one of the open problems in the *Swift* era, we do not manage this problem in this paper. Recently, the modern version of the reverse shock model was developed to explain the shallow decay emission in the early afterglow phase [67, 68]. In such models, the plateau shape can be achieved by requiring the appropriate distribution of Lorentz factors of the ejecta and the suppression of the forward shock emission. For the reverse shock emission to emerge in the x-ray band, we can consider a number fraction of the shocked electrons that are injected into the acceleration process f_e^r to be smaller than the unity. In this paper, we shall consider cosmic-ray acceleration in the early afterglow phase under the reverse shock model developed for the shallow decay emission, and adopt the small f_e^r following Refs. [35, 67].

The cosmic-ray production in the reverse shock model was discussed in Refs. [3, 31, 32]. The more detailed study can be found in Ref. [35]. As demonstrated in these references, cosmic-ray acceleration up to ultra-high energies at a reverse shock of HL GRBs is possible. In this paper, let us demonstrate that UHE cosmic-ray pro-

duction at a reverse shock of LL GRBs is also possible. First, $t_{\text{acc}} = t_{\text{dyn}} \approx t_{\text{ad}}$ leads to

$$(1+z)E_{N,\text{ad}}^{\text{max}} = \frac{ZeB_{\times}^r r_{\times}}{\eta} \simeq 4.7 \times 10^{20} \text{ eV } Z\eta^{-1} \times \epsilon_B^{1/2} E_{\text{ej},50}^{3/8} n_2^{1/8} T_3^{1/8}, \quad (12)$$

where T is the duration time measured by the observer in the local rest frame. Here, we have assumed the thick ejecta case, where the total ejecta thickness $\sim cT$ is larger than the shocked region at the crossing time $\sim r_{\times}/2\Gamma_0^2$. Here Γ_0 is the initial Lorentz factor. In the thin ejecta case, the corresponding expression can be derived easily. Second, $t_{\text{acc}} = t_{\text{syn}}$ leads to

$$(1+z)E_{N,\text{syn}}^{\text{max}} = \sqrt{\frac{6\pi Ze}{Z^4 \sigma_T B_{\times}^r \eta} \frac{\Gamma m_N^2 c^2}{m_e}} \simeq 1.3 \times 10^{21} \text{ eV } A^2 Z^{-3/2} \eta^{-1/2} \times \epsilon_B^{-1/4} E_{\text{ej},50}^{-3/16} n_2^{-5/16} T_3^{-1/16}. \quad (13)$$

Therefore, we can expect that UHECR production at a reverse shock is possible not only for HL GRBs but also LL GRBs. Note that even protons could be accelerated above 10^{20} eV unless ϵ_B is too small.

Photon spectra in the reverse shock model can be calculated by exploiting the reverse-forward shock model. For example, in the slow cooling regime ($\epsilon^m < \epsilon^{sa} < \epsilon^c$), we obtain

$$\frac{dn}{d\epsilon} = n_{\epsilon,\text{max}} \begin{cases} (\epsilon^{sa}/\epsilon^m)^{-\frac{p+1}{2}} (\epsilon^m/\epsilon^{sa})^{\frac{3}{2}} (\epsilon/\epsilon^m)^1 \\ (\epsilon^{sa}/\epsilon^m)^{-\frac{p+1}{2}} (\epsilon/\epsilon^{sa})^{\frac{3}{2}} \\ (\epsilon/\epsilon^m)^{-\frac{p+1}{2}} \\ (\epsilon^c/\epsilon^m)^{-\frac{p+1}{2}} (\epsilon/\epsilon^c)^{-\frac{p+2}{2}} \end{cases} \quad (14)$$

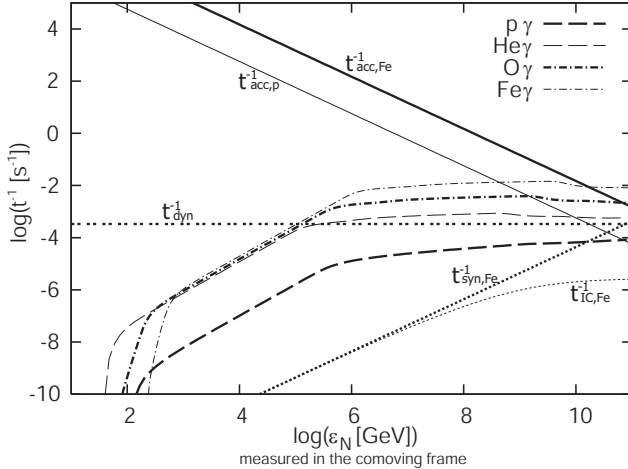


FIG. 4: The same as Fig. 3. But used parameters are $L_b = 10^{47} \text{ ergs s}^{-1}$, $\epsilon_{\text{ob}}^b = 5 \text{ keV}$, $\Gamma = 10$, $r = 9 \times 10^{14} \text{ cm}$ (corresponding to $\delta t/(1+z) = 150 \text{ s}$) and $\xi_B (\approx \epsilon_B/\epsilon_e) = 1$. Note that this parameter set is the same one as used in Ref. [14] and it implies that a moderate fraction of the energy carried by protons goes into neutrinos.

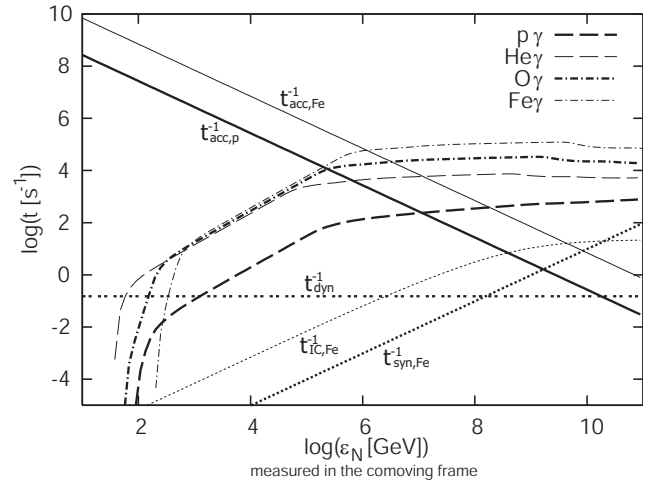


FIG. 5: The same as Fig. 3. But used parameters are $L_b = 10^{47} \text{ ergs s}^{-1}$, $\epsilon_{\text{ob}}^b = 5 \text{ keV}$, $\Gamma = 5$, $r = 7 \times 10^{12} \text{ cm}$, $l = 10^{11} \text{ cm}$ and $\xi_B (\approx \epsilon_B/\epsilon_e) = 1.1 \times 10^{-2}$. Note that this parameter set is the same one as used in Ref. [63] and it does not allow for accelerating cosmic rays up to ultra-high energies.

where [35, 43]

$$n_{\varepsilon, \max} = \frac{L_{\varepsilon, \max}}{4\pi r^2 c \varepsilon^n}. \quad (15)$$

Here $\varepsilon^n \equiv \min[\varepsilon^m, \varepsilon^c]$, and ε^m , ε^c and ε^{sa} are the injection energy, cooling energy and self-absorption energy in the comoving frame, respectively. $L_{\varepsilon, \max}$ is the comoving specific luminosity per unit energy at the injection or cooling energy. From Eq. (14), we can calculate t_{IC} and $t_{N\gamma}$.

We show the numerical result of the reverse shock model for LL GRBs in Fig. 7. The used parameters are $E_{ej} = 2 \times 10^{51}$ ergs, $n = 10^2 \text{ cm}^{-3}$, $\epsilon_e^r = \epsilon_B^r = 0.1$, $f_e^r = 0.025$, $T = 3000$ s and the initial Lorentz factor $\Gamma_0 = 5$. As seen in Fig. 7, the UHECR production is possible, where protons and Fe nuclei can be accelerated up to $\sim 10^{20.2}$ eV. But we cannot expect survival of UHE nuclei in this parameter set due to the copious photon field. For UHE nuclei accelerated above 10^{20} eV to survive, for example, much smaller ϵ_e^r is needed. If we adopt such parameters, we can expect both UHE protons and nuclei in this model.

C. Forward Shock Model

The expanding fireball strikes the surrounding medium and will form a forward shock. The self-similar behavior after the deceleration time t_{dec} is described by the Blandford-McKee solution. The standard external shock model based on this solution can reproduce observations at the late time. Although the original forward shock

model actually fails to explain the shallow decay emission, we consider the original forward shock model for simplicity. By exploiting the theory, we immediately have $\Gamma \propto t^{-3/8}$, $r \propto t^{1/4}$ and $B \propto t^{-3/8}$. By using them, we can derive the time-dependence of various quantities. Typical parameters for HL GRBs are $E_{ej} \sim 10^{52-53}$ ergs, $n = 1 \text{ cm}^{-3}$ (ISM), $\epsilon_B \sim 0.01$, $\epsilon_e \sim 0.1$ and $p \sim 2$. In obtaining above parameters, all the electrons are often assumed to be accelerated. However, this may not be true. As Eichler & Waxman [69] discussed, only a fraction f_e of electrons may be accelerated, that is, f_e can be smaller than the unity. When we consider the small f_e , the kinetic energy of ejecta can be larger by $1/f_e$. Such small values of f_e will be tested by observations of polarization in the future [70].

Cosmic-ray acceleration and neutrino production in the forward shock model for HL GRBs were discussed in detail by Dermer [33, 50]. Hereafter, let us demonstrate UHECR production at a forward shock for parameters of LL GRBs. In this paper, we shall adopt $E_{ej} = 2 \times 10^{51}$ ergs, $n = 10^2 \text{ cm}^{-3}$ (ISM), $\epsilon_B = 0.01$, $\epsilon_e = 0.01$, $f_e = 0.1$ and $p = 2$. This parameter set is consistent with parameters obtained by Toma et al. [64] except that we use $f_e = 0.1$.

Next, let us estimate maximum energies of cosmic rays. First, the maximum energy determined from the condition $t_{acc} = t_{dyn} \approx t_{ad} =$ is [35, 48, 49]

$$\begin{aligned} (1+z)E_{N,ad}^{\max} &= \frac{Ze\Gamma B^{\text{ISM}} r}{\eta} \\ &\simeq 7.1 \times 10^{14} \text{ eV } Z\eta^{-1} \\ &\times B_{-6}^{\text{ISM}} E_{ej,51}^{3/8} n_2^{-3/8} t_4^{1/8}. \end{aligned} \quad (16)$$

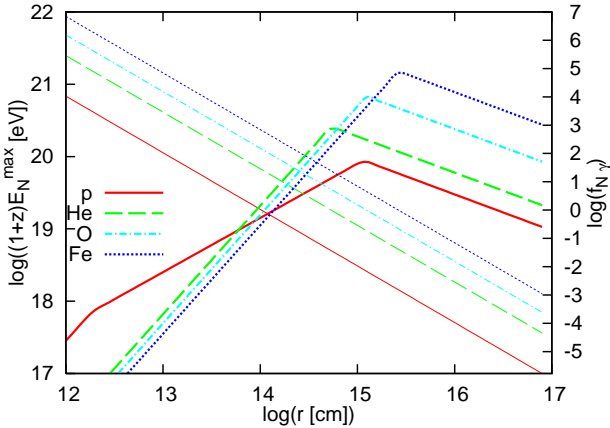


FIG. 6: The maximum energy of cosmic rays (thick lines) and the optical depth for photomeson production or photodisintegration (thin lines) as a function of the collision radius. Used parameters are $L_b = 1.5 \times 10^{46} \text{ erg s}^{-1}$, $\epsilon_{ob}^b = 5 \text{ keV}$, $\Gamma = 10$ and $\xi_B (\approx \epsilon_B/\epsilon_e) = 1$ for LL GRBs. The comoving shell width is set to $l = r/\Gamma$. Note that UHE nuclei can be produced in LL GRBs for $r \gtrsim 10^{15} \text{ cm}$. There, UHE nuclei can survive. At sufficiently large radii, E_N^{\max} becomes $E_{N,ad}^{\max}$.

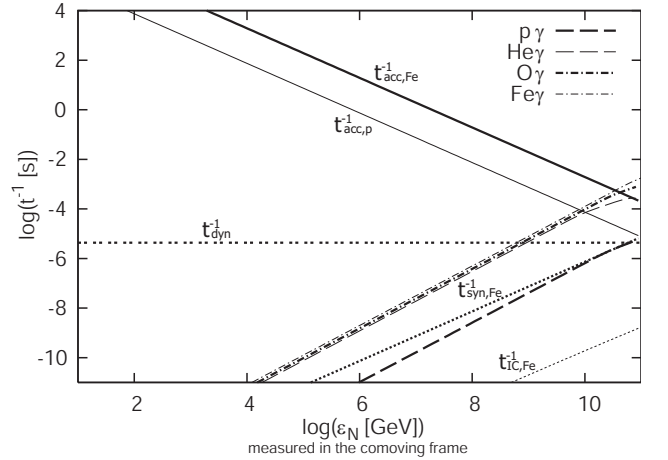


FIG. 7: The acceleration time scale and various cooling time scales of proton, helium, oxygen and iron in the reverse shock model for LL GRBs. Energy and time scales are measured in the comoving frame of the outflow. Used parameters are $E_{ej} = 2 \times 10^{51}$ ergs, $n = 10^2 \text{ cm}^{-3}$ (ISM), $\Gamma_0 = 5$, $T = 3 \times 10^3$ s, $\epsilon_B^r = 0.1$, $\epsilon_e^r = 0.1$, $f_e^r = 0.025$ and $p = 2.4$. Note that this parameter set does not allow for survival of UHE nuclei.

Here $(1+z)t$ is the time after the prompt emission measured by the observer. When we use the conventional value of the ISM magnetic field, we cannot expect UHECR production at a forward shock of GRBs. However, the magnetic field is likely to be amplified significantly via e.g., the non-resonant cosmic-ray streaming instability [33, 71] (but see also Ref. [72]). Instead, if the second-order Fermi acceleration works well [73], we could use the magnetic field in the downstream, which is likely to be amplified from observations. If the upstream and/or downstream magnetic fields are amplified up to near the equipartition value, $t_{\text{acc}} = t_{\text{dyn}} \approx t_{\text{ad}}$ leads to

$$(1+z)E_{N,\text{ad}}^{\text{max}} = ZeB^f r \eta^{-1} \simeq 2.7 \times 10^{20} \text{ eV } Z \eta^{-1} \times \epsilon_B^{1/2} E_{\text{ej},51}^{3/8} n_2^{1/8} t_4^{-1/8}. \quad (17)$$

The maximum energy limited by synchrotron cooling is

$$(1+z)E_{N,\text{syn}}^{\text{max}} = \sqrt{\frac{6\pi Ze}{Z^4 \sigma_T B^f \eta}} \frac{\Gamma m_N^2 c^2}{m_e} \simeq 2.5 \times 10^{20} \text{ eV } A^2 Z^{-3/2} \eta^{-1/2} \times \epsilon_B^{-1/4} E_{\text{ej},51}^{1/16} n_2^{-5/16} t_4^{-3/16}. \quad (18)$$

From Eqs. (17) and (18), we can expect that UHECR production is also possible at a forward shock of LL GRBs.

A photon spectrum in the forward shock model can be also calculated from the theory. For example, in the slow cooling case ($\epsilon^{sa} < \epsilon^m < \epsilon^c$), we have

$$\frac{dn}{d\epsilon} = \frac{L_{\epsilon,\text{max}}}{4\pi r^2 c \epsilon^n} \begin{cases} (\epsilon^{sa}/\epsilon^m)^{-\frac{2}{3}} (\epsilon/\epsilon^{sa})^1 \\ (\epsilon/\epsilon^m)^{-\frac{2}{3}} \\ (\epsilon/\epsilon^m)^{-\frac{p+1}{2}} \\ (\epsilon^c/\epsilon^m)^{-\frac{p+1}{2}} (\epsilon/\epsilon^c)^{-\frac{p+2}{2}} \end{cases} \quad (19)$$

Here, $\epsilon_{\text{ob}}^m = \Gamma \epsilon^m \simeq 0.17 \text{ eV } g_{-1}^2 f_{e,-1} \epsilon_{B,-2}^{1/2} \epsilon_{e,-1}^2 E_{\text{ej},51}^{1/2} t_4^{3/2}$, $\epsilon_{\text{ob}}^c = \Gamma \epsilon^c \simeq 1.0 \text{ eV } \epsilon_{B,-2}^{-3/2} E_{\text{ej},51}^{-1/2} n_2^{-1} t_4^{-1/2}$ and $L_{\epsilon_{\text{ob}},\text{max}} = \Gamma L_{\epsilon,\text{max}} \simeq 7.8 \times 10^{56} \text{ s}^{-1} f_{e,-1} \epsilon_{B,-2}^{1/2} E_{\text{ej},51}^{1/2} n_2^{1/2} (\phi_p/0.6)$, where ϕ_p is an order-of-unity factor calculated by Wijers & Galama [74].

The photodisintegration and/or photomeson cooling time scales are evaluated from Eqs. (3) and (4). Here, let us estimate these time scales analytically in the slow cooling case by applying Eq. (5). After replacing ϵ^b with ϵ^c , resonance approximations give

$$t_{N\gamma}^{-1} \simeq g_{-1} (\phi_p/0.6) \epsilon_{e,-2} \epsilon_{B,-2}^{3/2} E_{\text{ej},51}^{7/8} n_2^{13/8} t_4^{-5/8} \times \begin{cases} 1.1 \times 10^{-8} \text{ s}^{-1} & (\text{for } \Delta\text{-resonance}) \\ 5.7 \times 10^{-8} A^{1.21} \text{ s}^{-1} & (\text{for GDR}) \end{cases} \quad (20)$$

The above expressions are obtained for $E_N > E_N^b$. Hence, we have $f_{N\gamma} \propto t^{\frac{1}{8}}$ and $E_{N,N\gamma}^{\text{max}} \propto t^{-\frac{1}{8}}$ for $E_N > E_N^b$. Of course, the time-dependence differs for $E_N < E_N^b$. In the ISM case, we can see that $f_{N\gamma}$ increases with time. Note that the temporal index of $f_{N\gamma}$

is different from that used in Wang et al. [17], because we consider $E_N \sim 10^{20} \text{ eV}$, where $E_N > E_N^b$ is typically expected rather than $E_N < E_N^b$ considered by them.

In the wind-medium case, we have $E_{N,\text{ad}}^{\text{max}} \propto t^{-\frac{1}{4}}$ and $E_{N,\text{syn}}^{\text{max}} \propto t^{\frac{1}{8}}$. Furthermore, we can derive $E_{N,N\gamma}^{\text{max}} \propto t^{\frac{1}{2}}$ and $f_{N\gamma} \propto t^{-1}$ for $E_N > E_N^b$. In the wind-medium case, we can see that $f_{N\gamma}$ decreases with time. It is because the ambient density drops as r^{-2} , which leads to rapid drop of the photon density with time.

In the light curve of afterglows of HL GRBs, we can often find the jet break around $t_j \sim 10^5 \text{ s}$. After the jet break, we have $r \propto t^0$, $\Gamma \propto t^{-1/2}$ and $B \propto t^{-1/2}$. Therefore, we can derive $E_{N,\text{ad}}^{\text{max}} \propto t^{-\frac{1}{2}}$, $E_{N,\text{syn}}^{\text{max}} \propto t^{-\frac{1}{4}}$, $E_{N,N\gamma}^{\text{max}} \propto t^0$ and $f_{N\gamma} \propto t^{-\frac{1}{2}}$ for $E_N > E_N^b$. After the jet break, the photon density will become smaller and smaller. Hence, we expect photodisintegration and photomeson production become less important. Similarly, we can obtain the time-dependence of various quantities for the wind-medium case. In both cases, the effect of the jet break makes survival of UHE nuclei easier. It has not been pointed out in previous studies.

Results in the forward shock model for LL GRBs are shown in Figs. 8 and 9. In Fig. 8, we show maximum energies of cosmic rays E_N^{max} and the optical depth for photodisintegration $f_{N\gamma}$ at $E_N = 10^{20} \text{ eV}$ as a function of time t . From this figure, we can expect UHE nuclei can be produced at a forward shock of LL GRBs. For heavy nuclei (O and Fe), the photodisintegration cooling determines the maximum energy at the earlier time, but the adiabatic cooling becomes more important at the later time. For light nuclei, the adiabatic cooling is almost always the most important. Note that the jet-break effect can be important for survival of UHE nuclei, as expected. In fact, after the jet break, $f_{\text{Fe}\gamma}$ can decrease with time and become smaller than the unity.

In Fig. 9 we show the results for the wind-medium case. In this case, we also expect acceleration of UHECRs and survival of UHE nuclei. Since the photon density decreases with time, the maximum energy of heavy nuclei which is determined by $E_{N,N\gamma}^{\text{max}}$ can increase until the adiabatic cooling becomes more important. As a result, UHE nuclei could be accelerated up to $\gtrsim 10^{20} \text{ eV}$ in this parameter set.

III. ENERGETICS

In this section, let us briefly overview the energetics of GRBs and UHECRs in order to see that GRBs (and hypernovae) could be one of the candidates of UHECRs (despite of some caveats). The detailed arguments are found in Refs. [1, 2, 3, 7, 9, 22, 75, 76, 77, 78]. In the previous section, we have seen that relativistic outflows that make GRBs satisfy various conditions for cosmic rays to be accelerated up to greater than 10^{20} eV . Here, let us compare the energy generation rate of observed UHECRs with the gamma-ray energy generation

rate of GRBs. The UHECR generation rate given by Ref. [78] from Fly's Eye data is $E_{\text{CR}}^2 dN_{\text{CR}}/dE_{\text{CR}} \approx 0.65 \times 10^{44} \text{ ergs Mpc}^{-3} \text{ yr}^{-1}$. The UHECR generation rate from the recent PAO results [79] is compiled by Dermer [22]. The UHECR generation rate at 10^{19} eV is $E_{\text{CR}}^2 dN_{\text{CR}}/dE_{\text{CR}} \approx 0.8 \times 10^{44} \text{ ergs Mpc}^{-3} \text{ yr}^{-1}$. At higher energies, the value becomes smaller.

The radiation energy generation rate of GRBs is given by the product of the local GRB rate $\rho(0)$ (without the beaming-correction) and the average (isotropic equivalent) gamma-ray energy release E_{γ}^{iso} . First, let us consider HL GRBs. Recently, Kocevski & Butler [80] provided $E_{\gamma, [1\text{keV}, 10\text{MeV}]}^{\text{iso}} \sim (4.1 - 7.8) \times 10^{52} \text{ ergs}$, in a rest frame bandpass $(1 - 10^4) \text{ keV}$. Emission at higher energies (above the $(1 - 10^4) \text{ keV}$ band) implies that the total gamma-ray energy input can be even higher. Assuming $\beta \sim 2$, we can expect $E_{\gamma}^{\text{iso}} \sim (1 - 2) \times 10^{53} \text{ ergs}$. The energy input at high energies is rather uncertain, because it depends on the high-energy photon index, pair-creation cutoff and possible IC contribution. Here, we just adopt $3 \times 10^{53} \text{ ergs}$ as just a reference value for HL GRBs. On the other hand, by using logN-logS relationship with the assumption that the GRB rate traces, e.g., the star formation rate, various authors estimated the local GRB rate. In the pre-Swift era, the estimated long GRB rate was $\sim (0.2 - 1) \text{ Gpc}^{-3} \text{ yr}^{-1}$ (see, e.g., [13] and references there in). After the launch of *Swift*, many GRBs including high-redshift bursts were observed, and various authors provided the local GRB rate (see, e.g., [4, 5]). For example, Ref. [5] obtained $(0.2 - 0.3) \text{ Gpc}^{-3} \text{ yr}^{-1}$ assuming that the GRB rate traces the star formation rate.

However, some authors claimed that the GRB rate has a faster evolution with redshift, which leads to the lower local GRB rate, $\sim 0.05 \text{ Gpc}^{-3} \text{ yr}^{-1}$ [4, 5, 6]. Next, we shall consider LL GRBs. However, the radiation energy release and local rate of LL GRBs are much more uncertain. The radiation energy of GRB 060218 is $\sim 10^{50} \text{ ergs}$, while that of GRB 980425 is an order of magnitude smaller. The suggested local LL GRB rate is $\sim 10^{2-3} \text{ Gpc}^{-3} \text{ yr}^{-1}$ which are likely to be much higher than the local HL GRB rate [11, 12]. Note that we cannot exclude possibilities that there is no such a distinct population, although we assume the existence of LL GRBs in this paper. Too large rates would also be impossible due to constraints from observations of SNe Ibc. For example, Soderberg et al. [81] argued that at most $\sim 10\%$ of SNe Ibc are associated with off-beam LL GRBs based on their late-time radio observations of 68 local SNe Ibc.

Now, we can estimate the UHECR generation rate of GRBs from the radiation energy generation rate with an unknown baryon loading factor, which is defined by $U_{\text{CR}} \equiv \xi_{\text{acc}} U_{\gamma}$. Then, the cosmic-ray energy generation rate of GRBs can be written as $\mathcal{E}_{\text{CR}}^{\text{iso}} = \xi_{\text{acc}} E_{\gamma}^{\text{iso}} = \xi_{\text{acc}} (4\pi r^2 l) \Gamma U_{\gamma} N$. When we assume $p = 2$ as the source spectral index of UHECRs, the cosmic-ray energy generation rate at $10^{18.5-19.5} \text{ eV}$ is written as $E_{\text{CR}}^2 \frac{dN_{\text{CR}}}{dE_{\text{CR}}} = U_{\text{CR}}/R$, where R is defined as $R \equiv \ln(E_{\text{CR}}^{\text{max}}/E_{\text{CR}}^{\text{min}})$. The minimum energy is not well determined theoretically, but we can expect $E_N^{\text{min}} \sim \text{a few} \times \Gamma m_N c^2 \sim 10^{11.5} \text{ eV}$. We have also assumed that cosmic rays can be accelerated up to ultra-high energies, so that we can take $E_N^{\text{max}} \gtrsim 10^{20}$.

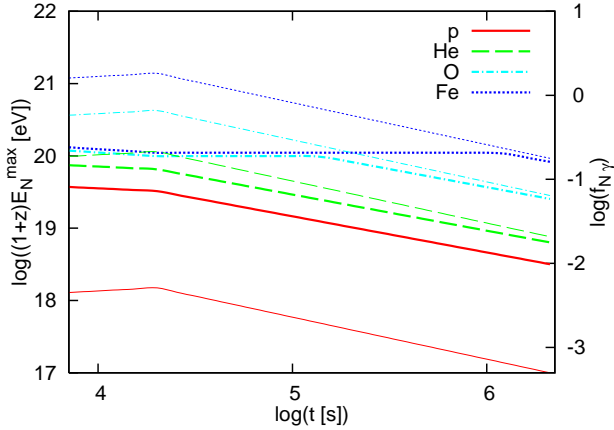


FIG. 8: The maximum energy of cosmic rays (thick lines) and the optical depth for photomeson production or photodisintegration at 10^{20} eV (thin lines) as a function of the time after the burst. Used parameters are $E_{\text{ej}} = 2 \times 10^{51} \text{ ergs}$, $n = 10^2 \text{ cm}^{-3}$ (ISM), $\epsilon_B = 0.01$, $\epsilon_e = 0.01$, $f_e = 0.1$ and $p = 2$. The jet-break time is set to $t_j = 2 \times 10^4 \text{ s}$. Note that the deceleration time is $t_{\text{dec}} \simeq 8000 \text{ s}$. UHE nuclei can be produced in a forward shock of LL GRBs. Survival of UHE nuclei becomes the most difficult at the jet-break time. At sufficiently late time, E_N^{max} becomes $E_{N,\text{ad}}^{\text{max}}$.

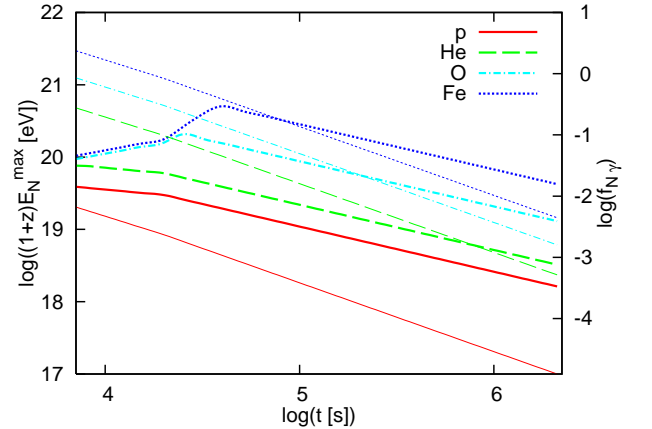


FIG. 9: The same as Fig. 8. But the wind-like circumburst medium is assumed ($A_* = 0.77$). UHE nuclei can be produced in a forward shock of LL GRBs. Survival of UHE nuclei becomes easier with time. At sufficiently late time, E_N^{max} becomes $E_{N,\text{ad}}^{\text{max}}$.

eV. Hence, for HL-GRBs, we obtain [82]

$$E_{\text{CR}}^2 \frac{d\dot{N}_{\text{CR}}}{dE_{\text{CR}}} = 3.0 \times 10^{43} \text{ ergs Mpc}^{-3} \text{ yr}^{-1} \left(\frac{\xi_{\text{acc}}}{10} \right) \left(\frac{20}{R} \right) \times \left(\frac{E_{\gamma}^{\text{iso}}}{3 \times 10^{53} \text{ ergs}} \right) \left(\frac{\rho_{\text{HL}}(0)}{0.2 \text{ Gpc}^{-3} \text{ yr}^{-1}} \right). \quad (21)$$

and for LL GRBs,

$$E_{\text{CR}}^2 \frac{d\dot{N}_{\text{CR}}}{dE_{\text{CR}}} = 5.0 \times 10^{43} \text{ ergs Mpc}^{-3} \text{ yr}^{-1} \left(\frac{\xi_{\text{acc}}}{10} \right) \left(\frac{20}{R} \right) \times \left(\frac{E_{\gamma}^{\text{iso}}}{2 \times 10^{50} \text{ ergs}} \right) \left(\frac{\rho_{\text{LL}}(0)}{500 \text{ Gpc}^{-3} \text{ yr}^{-1}} \right) \quad (22)$$

Therefore, the UHECR energy generation rate is roughly comparable to the radiation energy generation rate of GRBs (unless, for example, we use the smaller local GRB rate inferred from the faster evolution with redshift). In other words, we can expect $E_{\text{CR}}^2 \frac{d\dot{N}_{\text{CR}}}{dE_{\text{CR}}} (10^{19} \text{ eV}) \sim \epsilon_{\text{ob}}^2 \frac{d\dot{N}_{\gamma}}{d\epsilon_{\text{ob}}} (\epsilon_{\text{ob}}^b)$ for both of HL GRBs and LL GRBs, and two populations can supply the necessary amount of UHECRs, when $\xi_{\text{acc}} \sim 10$ and $p \sim 2$. From Eq. (21), we may have the required baryon loading factor $\xi_{\text{acc}} \gtrsim 20$ for HL GRBs, which is consistent with Ref. [22]. However, it is not a solid value and smaller ξ_{acc} could be possible, because the local GRB rate (and the total radiation energy input and the minimum cosmic-ray energy) is not so certain, and we may expect that GRB is one of the UHECR candidates at present.

In the reverse-forward and/or hypernova models, we usually use the kinetic energy of ejecta instead of the radiation energy of the prompt emission. The nonthermal cosmic-ray energy is written as $\mathcal{E}_{\text{CR}} \equiv \epsilon_{\text{acc}} E_{\text{ej}}$. In the case of supernova, $\epsilon_{\text{acc}} \gtrsim 0.1$ is needed to explain the cosmic-ray flux below the knee. From observations of afterglows, we typically have $E_{\text{ej}} \sim 10^{52-53}$ ergs for HL GRBs, while $E_{\text{ej}} \sim 10^{50-51}$ ergs for LL GRBs. In the hypernova model, the total kinetic energy of the hypernova ejecta, $E_{\text{ej}} \sim 5 \times 10^{52}$ ergs is expected (see [16] and references there in). But note that UHECRs can be produced only in the high velocity ejecta with $\Gamma\beta \gtrsim 0.5$, which carries $E_{\text{ej}} \sim 2 \times 10^{51}$ ergs [16, 17]. For these models, instead of Eq. (22), we have

$$E_{\text{CR}}^2 \frac{d\dot{N}_{\text{CR}}}{dE_{\text{CR}}} = 4.0 \times 10^{43} \text{ ergs Mpc}^{-3} \text{ yr}^{-1} \epsilon_{\text{acc}} \left(\frac{25}{R} \right) \times \left(\frac{E_{\text{ej}}^{\text{iso}}}{2 \times 10^{51} \text{ ergs}} \right) \left(\frac{\rho_{\text{LL}}(0)}{500 \text{ Gpc}^{-3} \text{ yr}^{-1}} \right) \quad (23)$$

Hence, UHECRs could be explained in the external shock model and/or hypernova model for LL GRBs as well as the external shock model for HL GRBs. A significant fraction of the kinetic energy must be injected to the nonthermal cosmic-ray energy. As in the case of supernovae, $\epsilon_{\text{acc}} \sim 1$ will be required. Note that the hypernova model is originally considered in order to explain

high-energy cosmic rays above the second knee, where the cosmic-ray spectrum is formed by the superposition of cosmic-rays from hypernova ejecta with various velocities. The velocity profile with $dE_{\text{ej}}/d(\Gamma\beta) \propto (\Gamma\beta)^{-2}$ leads to the superposed spectral index 3. In order to explain UHECRs above the ankle, we would need some additional reason (which was not given in Refs. [16, 17]), such as, e.g., the variable index of the velocity profile or the velocity-dependent baryon loading.

The above estimates are based on the assumption that the source spectral index is $p = 2.0$. However, if it is steeper, the required energy generation rate becomes much larger. In the dip model suggested by [9, 10], the typical spectral index is $p \sim 2.4$, which is steeper than $p \sim 2.2$ in the ankle model. Such a steep spectrum leads to the larger baryon loading factor, unless we change $E_{\text{CR}}^{\text{min}}$. For example, we have $R(10^{19} \text{ eV}) \equiv \mathcal{E}_{\text{CR}} / (E_{\text{CR}}^2 \frac{d\dot{N}_{\text{CR}}}{dE_{\text{CR}}}(10^{19} \text{ eV})) \sim 2500$ for $p = 2.4$ and $E_{\text{CR}}^{\text{min}} \sim 10^{11.5} \text{ eV}$, which can be obtained easily from its definition. Furthermore, we have neglected the cosmic-ray energy loss at the source. For example, the efficient neutrino production leads to depletion of high-energy cosmic rays if the shock dissipation at sufficiently inner radii. When $f_{p\gamma}$ is not small, the required nonthermal cosmic-ray energy will be raised by $\sim 1/(1 - f_{p\gamma})$. In addition, the adiabatic loss and escape of particles should be taken into account for more realistic calculations.

From Eqs. (21), (22) and (23), we expect that GRBs can be the main UHECR sources in both of the internal shock model, and the external reverse and forward shock model. However, note that too large nonthermal baryon loading factors seem implausible because the available energy for nonthermal cosmic rays would be limited, e.g., by gravitational energy of falling materials of massive stars. In addition, the high radiative efficiency of the prompt emission [83] might infer that the large baryon loading is impossible, as long as the nonthermal baryon energy is smaller than the thermal baryon energy. Although these possible caveats, current theories cannot answer whether efficient UHECR production in GRBs is possible or not. Rather, we should test this GRB-hypothesis from observations. Current and future observations of UHECRs, neutrinos and gamma rays will give us useful information. For example, observations by AMANDA and IceCube have enabled us to constrain the averaged value of $f_{p\gamma}$ under the GRB-UHECR hypothesis [84, 85]. In the following sections, we discuss various implications to multi-messenger astronomy.

IV. IMPLICATIONS TO COSMIC-RAY ASTRONOMY

The discussions toward UHECR astronomy have been recently begun. The direct correlation between UHECR sources and observed UHECR arrival directions is one of the approaches to study the source properties. This can be expected only if the deflection angle due to the galac-

tic magnetic field (GMF) and EGMF is small enough. The latter is poorly known both theoretically and observationally. 95% of volume within 100 Mpc can be regarded as the void region, whose uniform magnetic field is not well-known. The Faraday rotation measurement of radio signals from distant quasars implies $B_{\text{EG}}^{\text{void}} \lambda_{\text{Mpc}}^{1/2} \lesssim 10^{-9} \text{ GMpc}^{1/2}$ [86, 87]. In addition, there is also the structured EGMF which traces the local matter distribution. Observationally, clusters of galaxies have strong magnetic fields with $(0.1 - 1) \mu\text{G}$ at its center. This structured EGMF is very important for UHECR propagation (see, e.g., [88, 89] and references there in). The GMF is relatively well measured, but the magnetic field of the galactic halo is not known well. This GMF also affects trajectories of UHECRs [90]. If UHECR trajectories are deflected only weakly, the deflection angle by EGMF can be written as

$$\begin{aligned} \theta_d &\approx \frac{\sqrt{2}ZeB_{\text{EG}}D}{3E_N\sqrt{D/\lambda}} \\ &\simeq 2.5^\circ Z_1 E_{N,20}^{-1} B_{\text{EG},-10} \lambda_{\text{Mpc}}^{1/2} D_{100 \text{ Mpc}}^{1/2} \end{aligned} \quad (24)$$

$$\begin{aligned} \theta_d &\approx \frac{ZeB_{\text{EG}}D}{2E_N} \\ &\simeq 2.6^\circ Z_1 E_{N,20}^{-1} B_{\text{EG},-11} D_{100 \text{ Mpc}}. \end{aligned} \quad (25)$$

Eq. (25) is for the coherent EGMF ($\theta_s D \ll \lambda$), while Eq. (24) is for the EGMF with the coherent length λ ($\theta_s D \gg \lambda$). Recent PAO results imply the $\sim 3^\circ$ deflection angle, assuming that nearby AGN are UHECR sources [20, 21]. The inferred value $B_{\text{EG}} \sim 10^{-10} \text{ G}$ is consistent with the predicted EGMF strength, and it could be used to set lower limits on the mean EGMF [22]. However, in fact, we cannot neglect the effect of the GMF. Although the deflection angle due to the GMF depends on the model of the galactic magnetic field, it can become $\gtrsim 3^\circ$. Therefore, lower limits could be set only if we see the direction where the effect of the GMF is small. In addition, the inferred value is derived from the positional correlation between the arrival directions of UHECRs and the incomplete AGN catalogue used by the PAO collaboration. Therefore, in general, more observations and careful examinations are required in order to estimate the mean EGMF.

Although the GMF can be important for the deflection angle, it does not affect the delayed time so much. From Eqs. (24) and (25), we can estimate the delayed time of UHECRs as

$$\begin{aligned} \tau_d &\approx \frac{D\theta_d^2}{6c} \simeq 10^3 \text{ yrs } Z^2 E_{N,20}^{-2} \\ &\times B_{\text{EG},-10}^2 \lambda_{\text{Mpc}} D_{100 \text{ Mpc}}^2 \end{aligned} \quad (26)$$

$$\begin{aligned} \tau_d &\approx \frac{D\theta_d^2}{2c} \simeq 3.5 \times 10^3 \text{ yrs } Z^2 E_{N,20}^{-2} \\ &\times B_{\text{EG},-11}^2 D_{100 \text{ Mpc}}^3. \end{aligned} \quad (27)$$

Eq. (27) is for the coherent EGMF, while Eq. (26) is for the EGMF with coherent length λ . Later we shall use the

former expression for convenience. Note that the EGMF in the above equations expresses the mean EGMF field. UHE protons suffer from the stochastic energy loss due to photomeson production above the GZK energy, so that the dispersion of the arrival time is also $\sim \tau_d$. As long as we can use Eq. (26), we also expect multiplets such that the lower energy cosmic-ray event precede higher energy cosmic-ray event, because the time delay is statistically distributed [77].

From the delayed time and observed local GRB rate, we can estimate the number density of GRB-UHECR sources. Let us perform a simple analytic calculation for the number density of GRB-UHECR sources. Following Ref. [91], we adopt the top-hat model, where the effect of energy losses are approximately negligible when $D < D_c(E_{\text{CR}})$, and eliminating all cosmic rays coming from $D > D_c(E_{\text{CR}})$. Here, $D_c(E_{\text{CR}})$ is the effective cutoff distance. For example, we obtain $D_c(E_p = 10^{20} \text{ eV}) \approx 50 \text{ Mpc}$ when we define that $D_c(E_{\text{CR}})$ is the radius from which $1/e$ of cosmic rays can reach us (see, e.g., [93]). By assuming that we can observe GRB-UHECR sources only during the duration time which is comparable to the delayed time $\sim \tau_d$, we have

$$F_{\text{CR}} \approx \frac{1}{4\pi D^2 \tau_d} \frac{dN_{\text{CR}}}{dE_{\text{CR}}}, \quad (28)$$

where F_{CR} is the observed UHECR flux at a given energy. Most cosmic rays above the effective cutoff radius D_c cannot reach us. Hence, the minimum flux F_{CR}^c for a given $\frac{dN_{\text{CR}}}{dE_{\text{CR}}}$ is obtained by substituting D_c into D . We also have the corresponding delayed time τ_d^c . The number density of GRB-UHECR sources at UHE energies is calculated by integrating the differential source number density (the number of GRBs per unit observed UHECR flux) over the UHECR flux $F_{\text{CR}} \gtrsim F_{\text{CR}}^c$. As a result, we have $n_s \approx (3/5)\rho(0)\tau_d^c$. Note that, in the GRB-UHECR hypothesis, the number density of UHECR sources will depend on the observed energy because τ_d^c depends on the energy. The number density of GRB-UHECR sources observed at $E_p = 10^{19.9} \text{ eV}$ becomes

$$\begin{aligned} n_s^{\text{HL}} &\approx \frac{3}{5} \rho_{\text{HL}}(0) \tau_d^c \simeq 1.1 \times 10^{-5} \text{ Mpc}^{-3} B_{\text{EG},-9}^2 \lambda_{\text{Mpc}} \\ &\times \left(\frac{\rho_{\text{HL}}(0)}{0.2 \text{ Gpc}^{-3} \text{ yr}^{-1}} \right) \end{aligned} \quad (29)$$

$$\begin{aligned} n_s^{\text{LL}} &\approx \frac{3}{5} \rho_{\text{LL}}(0) \tau_d^c \simeq 2.8 \times 10^{-5} \text{ Mpc}^{-3} B_{\text{EG},-10}^2 \lambda_{100 \text{ pc}} \\ &\times \left(\frac{\rho_{\text{LL}}(0)}{500 \text{ Gpc}^{-3} \text{ yr}^{-1}} \right). \end{aligned} \quad (30)$$

The number density of UHECR sources for arbitrary energies can be obtained by calculating D_c^2/E_{CR}^2 . Eqs. (29) and (30) suggest that determination of the number density of UHECR sources and mean EGMF enable us to test the GRB-UHECR hypothesis. The latter is especially not easy, hence one of the ultimate goals of the UHECR astronomy. But future observations of UHECRs by PAO and TA will give us clues to them.

The source number density can be estimated from the study of the small-scale anisotropy. If the observed small-scale clustering originates in the same sources, we can estimate the minimum number density of UHECR sources [94, 95]. For example, recent PAO observations showed 6 pairs with separation smaller than the correlation angle scale of 6° among the 27 highest-energy events. This leads to a lower limit for the number of sources ≥ 61 [21]. When we adopt $D_c \approx 130$ Mpc, we can estimate the source number density as $n_s \gtrsim 3 \times 10^{-5} \text{ Mpc}^{-3}$. In more detail, the significance of small-scale clustering in the arrival directions of UHECRs can be studied by the angular two-point auto-correlation function. By simulating the arrival distribution of UHECRs, the source number density that can reproduce observational results can be estimated [96]. The constraint obtained from the small-scale anisotropy observed by AGASA is $n_s \gtrsim 10^{-5} \text{ Mpc}^{-3}$ for uniformly distributed proton sources. Despite large uncertainties due to a small number of observed events, PAO observations in the future can lead to the more robust estimation [97].

For example, if we can find that the source number density is $n_s \sim 10^{-4} \text{ Mpc}^{-3}$, the required mean EGMF for a given local GRB rate is $B_{\text{EG},-9}^2 \lambda_{\text{Mpc}} \sim 9$ (which is larger the upper limit of the uniform EGMF) for HL GRBs and $B_{\text{EG},-9}^2 \lambda_{\text{Mpc}} \sim 0.004$ for LL GRBs. However, since the robust estimation of the source number density may be difficult, we may have only the lower limit. In such cases, for example, $n_s \gtrsim 10^{-5} \text{ Mpc}^{-3}$ would infer the required EGMF $B_{\text{EG},-9}^2 \lambda_{\text{Mpc}} \gtrsim 0.9$ for HL GRBs and $B_{\text{EG},-9}^2 \lambda_{\text{Mpc}} \gtrsim 0.0004$ for LL GRBs. Therefore, determination of the upper limit on the mean EGMF is important in order to test the GRB-UHECR hypothesis. If we know that the mean EGMF is too weak, possibilities of HL GRBs as observed main UHECR sources could be excluded. (However, we could still expect to see HL GRBs as rare but very bright UHECR sources. In such cases, one HL GRBs could be found as a very bright event among $\sim \rho_{\text{LL}}(0)/\rho_{\text{HL}}(0) \sim 1000$ LLGRB-UHECR sources.) On the other hand, when the mean EGMF is strong enough, HL GRBs rather than LL GRBs would be more plausible main UHECR sources. It is because the too large source number density cannot explain the anisotropy [97]. Of course, when LL GRBs can also produce UHECRs, they could be regarded as numerous faint sources, and it is difficult to exclude the existence of such faint sources. More generally, we should employ the luminosity-weighted distribution rather than the luminosity-uniform distribution. Even if LL GRBs do not form a distinct population, it would be important to know the local GRB rate as a function of E_γ^{iso} for more refined investigations.

Although Eqs. (29) and (30) suggest that future observations enable us to test the GRB-UHECR hypothesis, the above estimation is simple and not quantitative. In order to present realistic arguments, we need the detailed simulation of cosmic-ray propagation, which is beyond scope of this paper. In addition, we have assumed that

UHECRs are protons. When UHECRs are heavier nuclei, τ_d^c for heavy nuclei differs from that for protons, so that the source number density also depends on the composition of UHECRs.

Before finishing this section, let us briefly describe observable features which are expected for GRB-UHECR sources. In the GRB-UHECR model, we can expect several prominent features different from those in the steady source models. One can be observed in the clustering properties. Since the UHECR flux is proportional to D^{-4} as seen in Eq. (28), the differential source number density is proportional to $F_{\text{CR}}^{-9/4}$ as long as we assume the luminosity-uniform source distribution [91]. This leads to the source number density above F_{CR} is proportional to $F_{\text{CR}}^{-5/4}$, which differs from the steady source model where we have $\propto F_{\text{CR}}^{-3/2}$. This difference leads to the difference in the average number of multiplets, i.e., the difference in the ratio of the expected number of clusters with different multiplicities [95]. In the GRB-UHECR model, we may obtain the ratio between the number of triplets or higher multiplets and doublets, which is ~ 0.6 in the GRB-UHECR model, while ~ 0.33 in the steady source model.

Another prominent feature is the existence of the critical energy [91]. As seen in Eqs. (29) and (30), the source number density decreases with the energy. Since D_c decreases rapidly above the pion production threshold energy, τ_d^c will also show the rapid decrease above the pion threshold energy. Therefore, there exists the critical energy where the observed source number becomes the unity. Around this critical energy, we have possibilities to see the considerably higher flux than time-averaged UHECR flux from all sources. For the source number density $n_s = 10^{-5} \text{ Mpc}^{-3}$, we expect $E_c \sim 1.4 \times 10^{20}$ eV for proton sources. For $n_s = 10^{-4} \text{ Mpc}^{-3}$, $E_c \sim 2.5 \times 10^{20}$ eV is expected.

V. IMPLICATIONS TO NEUTRINO ASTRONOMY

As seen in Sec. II, sufficiently high-energy cosmic rays cannot avoid the photomeson production process, where the pion production threshold energy is 145 MeV. Generated pions, kaons and other mesons can produce high-energy neutrinos. Such high-energy neutrino signals, if detected, are very important as a direct probe of cosmic-ray acceleration. High-energy neutrino emission from accelerated protons at shocks was predicted by Waxman & Bahcall [30] in the internal shock model. Predictions were also done in the reverse-forward shock model [31, 32, 33]. Further predictions in the *Swift*-era are found in Refs. [14, 34, 35].

The important quantity for the neutrino flux is the effective optical depth for the photomeson process $f_{p\gamma}$, which also represents an energy fraction of protons carried by mesons, as long as $f_{p\gamma} < 1$. When $f_{p\gamma} \gtrsim 1$, accel-

erated protons are depleted by photomeson production, which also means the efficient photomeson production. Such conditions are satisfied when internal shocks making the prompt emission occur at sufficiently small radii [8]. In addition, $f_{p\gamma} \gtrsim 1$ is also possible in the case of flares and late prompt emissions [34, 35].

On the other hand, when $f_{p\gamma} \lesssim 1$, high-energy protons can survive without complete depletion. Such conditions are satisfied when internal shocks making prompt emission occur at sufficiently large radii. In the reverse-forward shock model (with the ISM environment), $f_{p\gamma} \lesssim 1$ is usually expected except in the highest-energies. However, we still expect that a significant fraction of the non-thermal proton energy is released as neutrinos unless $f_{p\gamma}$ is too small [31, 33, 35].

However, high-energy neutrino detection is not easy, and especially difficult to see neutrino signals from one GRB event. Hence, we need to see cumulative neutrino events as the neutrino background. Since HL GRBs are bright in the gamma-ray energy range, we expect the coincidence between neutrinos and gamma rays, which enables us to neglect the atmospheric neutrino background and cosmogenic neutrino background. On the other hand, neutrino signals from LL-GRBs are very dim in the sense that most of the neutrino signals will not correlate with photon signals. Only for very nearby bursts, we might be able to expect such correlations, and it requires many-years operations. However, we may see neutrino events that are positionally correlated with SNe Ic associated with LL-GRBs. The angular resolution of IceCube for neutrinos is about 1 degree or so, which might be searched by the optical-infrared follow-ups with ground-based optical telescopes.

In most previous works, all the cosmic rays are assumed to be protons. However, heavier nuclei may be entrained, which can also be accelerated up to ultra-high energies as shown in this paper. In the mixed composition model, the neutrino flux will deviate from that in the proton model, as demonstrated in Ref. [98]. The detailed study of the neutrino flux is beyond scope of this paper and one of our future works. Here, let us consider simple cases where UHE nuclei can survive, $f_{N\gamma} < 1$. First, note that we can relate $f_{p\gamma}$ with $f_{N\gamma}$ as

$$\frac{f_{p\gamma}(E_N)}{f_{N\gamma}(E_N)} \simeq 0.2A^{-1.21} \begin{cases} E_N^{\beta-\alpha} (E_p^b)^{1-\beta} (E_N^b)^{\alpha-1} \\ (E_N^b/E_p^b)^{\alpha-1} \end{cases} \quad (31)$$

Here, the parameter regions for the upper and lower columns are $E_N < E_p^b$ and $E_N \geq E_p^b$, respectively. From Eq. (31), we can see that $f_{p\gamma}$ is very small at radii where heavy nuclei can survive $f_{N\gamma} < 1$. If protons are dominant enough there, the neutrino emission is less expected. More generally, the amount of neutrinos depends on the composition, because not only protons but also UHE nuclei can produce neutrinos via the photomeson production process. The cross section of photomeson production for heavy nuclei is roughly expressed as $\sigma_{\text{meson}} \simeq A^{2/3} \sigma_{\Delta}$. Therefore, we can expect that neutrinos from UHE nuclei

give more contributions than those from UHE protons, when UHE nuclei are dominant rather than UHE protons.

One of the most promising neutrino signals is cosmogenic neutrino. It is difficult to use these neutrinos for identification of the source. These neutrinos will be observed as just the neutrino background. However, recent studies have suggested that GRBs may have the strong evolution with redshifts. The strong evolution of UHECR sources leads to the higher cosmogenic neutrino flux, which may be useful as one of the clues to the GRB-UHECR hypothesis [99]. In addition, these neutrino signals can give us information on the source spectral index, that is, they are useful to distinguish the ankle model from the dip model [100, 101].

A. Internal Shock Model

The most frequently discussed neutrino emission phase is the prompt emission one, based on the internal shock model. Since the prediction by Waxman & Bahcall [30], high-energy neutrino spectra have been calculated by various authors. We can evaluate $f_{p\gamma} \equiv t_{\text{dyn}}/t_{p\gamma}$ analytically by using the Δ -resonance approximation [30, 34]. For HL GRBs, we obtain

$$f_{p\gamma} \simeq 0.3 \frac{L_{b,51.5}}{r_{14} \Gamma_{2.5}^2 \epsilon_{\text{ob},316 \text{ keV}}^b} \begin{cases} (E_p/E_p^b)^{\beta-1} & (E_p < E_p^b) \\ (E_p/E_p^b)^{\alpha-1} & (E_p^b < E_p) \end{cases} \quad (32)$$

Here we have multiplied a factor of ~ 2.5 due to the effect of the multi-pion production which is important for $\alpha \sim 1$ spectra [34]. For LL GRBs, we have [14]

$$f_{p\gamma} \simeq 0.06 \frac{L_{b,47}}{r_{15} \Gamma_1^2 \epsilon_{\text{ob},5 \text{ keV}}^b} \begin{cases} (E_p/E_p^b)^{\beta-1} & (E_p < E_p^b) \\ (E_p/E_p^b)^{\alpha-1} & (E_p^b < E_p) \end{cases} \quad (33)$$

By using $f_{p\gamma}$ evaluated from the above equations, the diffuse neutrino background can be calculated for a given cosmology (e.g., the standard Λ CDM cosmology with $\Omega_m = 0.3, \Omega_\Lambda = 0.7; H_0 = 71 \text{ km s}^{-1} \text{ Mpc}^{-1}$). The diffuse neutrino flux from HL GRBs can be approximately evaluated by the following analytical expression [34, 102],

$$\begin{aligned} E_\nu^2 \Phi_\nu &\sim \frac{c}{4\pi H_0} \frac{1}{4} \min[1, f_{p\gamma}] E_p^2 \frac{dN_p^{\text{iso}}}{dE_p} \rho_{\text{HL}}(0) f_z \\ &\simeq 2 \times 10^{-9} \text{ GeV cm}^{-2} \text{ s}^{-1} \text{ str}^{-1} \left(\frac{\xi_{\text{acc}}}{10} \right) E_{\gamma,53}^{\text{iso}} \\ &\times \left(\frac{f_{p\gamma}}{0.3} \right) \left(\frac{\rho_{\text{HL}}(0)}{0.2 \text{ Gpc}^{-3} \text{ yr}^{-1}} \right) \left(\frac{f_z}{3} \right), \end{aligned} \quad (34)$$

and for LL GRBs we have [14]

$$\begin{aligned}
E_\nu^2 \Phi_\nu &\sim \frac{c}{4\pi H_0} \frac{1}{4} \min[1, f_{p\gamma}] E_p^2 \frac{dN_p^{\text{iso}}}{dE_p} \rho_{\text{LL}}(0) f_z \\
&\simeq 7 \times 10^{-10} \text{GeVcm}^{-2} \text{s}^{-1} \text{str}^{-1} \left(\frac{\xi_{\text{acc}}}{10} \right) E_{\gamma,50}^{\text{iso}} \\
&\times \left(\frac{f_{p\gamma}}{0.05} \right) \left(\frac{\rho_{\text{LL}}(0)}{500 \text{Gpc}^{-3} \text{yr}^{-1}} \right) \left(\frac{f_z}{3} \right), \quad (35)
\end{aligned}$$

where f_z is the correction factor for the possible contribution from high redshift sources, which depends on the cosmology. Expected muon events by IceCube are $N_\mu \sim 10$ events/yr for HL GRBs and $N_\mu \sim 5$ events/yr for LL GRBs. As we can see from Eqs. (34) and (35), the diffuse neutrino flux depends on $\min[1, f_{p\gamma}]$. For HL GRBs, we typically expect $\min[1, f_{p\gamma}] \sim (0.01 - 1)$. Smaller values are possible only at larger radii and/or for larger Lorentz factors. If UHE nuclei can survive, values of $f_{p\gamma}$ should be further small, $f_{p\gamma} \sim 10^{-3}$. As shown later, such parameter ranges also correspond to those allowing for the TeV gamma-ray emission. Since they may be rather constrained (see also [103]), we may not typically expect survival of UHE nuclei for HL GRBs.

Next, let us estimate the neutrino flux in cases where UHE nuclei can survive. Generally, results depend on the composition. If protons are dominant, high-energy neutrinos from protons make a main contribution compared to other nuclei. In addition, if $f_{\text{Fe}\gamma} < 1$, we see that the detection of neutrinos by IceCube is difficult from Eqs. (31), (34) and (35). If a significant fraction of cosmic rays are UHE nuclei rather than UHE protons, neutrinos mainly come from UHE nuclei. The neutrino flux can be estimated by using f_{meson} , which is given by the cross section of photomeson production of heavy nuclei as

$$f_{\text{meson}} \simeq 1.4 \times 10^{-3} \frac{A^{2/3} L_{b,46.2}}{r_{15.8} \Gamma_1^2 \varepsilon_{\text{ob},5 \text{keV}}^b} \begin{cases} (E_N/E_N^b)^{\beta-1} \\ (E_N/E_N^b)^{\alpha-1} \end{cases} \quad (36)$$

Here, the parameter regions for the upper and lower columns are $E_N < E_N^b$ and $E_N \geq E_N^b$, respectively. For example, when $f_{\text{Fe}\gamma} \sim 0.6$ as demonstrated in Fig. 3, we have $f_{p\gamma} \sim 8 \times 10^{-4}$ and $f_{\text{meson,Fe}} \sim 10^{-4}$. As a result, the expected diffuse neutrino flux is $E_\nu^2 \Phi_\nu \lesssim 10^{-10} \text{GeVcm}^{-2} \text{s}^{-1} \text{sr}^{-1}$ for this parameter set. The expected muon event rates are small, $N_\mu \lesssim 1$ event/yr.

B. Reverse-Forward Shock Model

In the reverse-forward shock model as well as the internal shock model, neutrino signals are expected. The neutrino emission in the early afterglow phase was studied in detail in Refs. [35, 50]. We can evaluate the photomeson production efficiency as [35]

$$f_{p\gamma} \simeq 0.088 \frac{L_{b,48}}{r_{16} \Gamma_2^2 \varepsilon_{\text{ob},10 \text{eV}}^b} \begin{cases} (E_p/E_p^b)^{\beta-1} & (E_p < E_p^b) \\ (E_p/E_p^b)^{\alpha-1} & (E_p^b < E_p) \end{cases} \quad (37)$$

where $\varepsilon_{\text{ob}}^b$ is $\varepsilon_{\text{ob}}^m$ or $\varepsilon_{\text{ob}}^c$ or $\varepsilon_{\text{ob}}^{sa}$. In the reverse-forward shock model, we typically obtain $f_{p\gamma} < 1$ except in the highest energies. The typical neutrino energy is around $\sim 10^{18}$ eV rather than $\sim 10^{15}$ eV (which is expected for the prompt emission). Hence, expected muon event rates by IceCube are generally small, and the detection is not so easy even by other detectors such as PAO. Nevertheless, since EeV neutrinos are produced by $\sim 10^{20}$ eV protons, the detection of such very high-energy neutrinos is useful for diagnosing UHECR acceleration at acceleration sites. (For the prompt emission, the typical neutrino energy is $\sim \text{PeV}$, and PeV neutrinos are produced by protons with $\sim 10^{17}$ eV, smaller than ultra-high energies.)

Next, let us consider the forward shock model. From Eq. (37) and various quantities derived under the forward shock model, we can obtain the photomeson production efficiency. By replacing ε^b and L_b with $\varepsilon_{\text{ob}}^c$ and $\Gamma^2(\varepsilon^c \varepsilon^m)^{1/2} L_{\varepsilon, \text{max}}$, respectively, we have

$$f_{p\gamma} \simeq 2.1 \times 10^{-2} g_{-1} \epsilon_{e,-1} \epsilon_{B,-1}^{3/2} E_{\text{ej},53} n_0^{3/2} \begin{cases} (E_p/E_p^b)^1 \\ (E_p/E_p^b)^{0.5} \end{cases} \quad (38)$$

As seen in the previous section, $f_{p\gamma}$ increases with time in the ISM case (before the jet break), while decreases in the wind-medium case. For example, when we assume $\epsilon_{\text{acc}} E_{\text{ej}} = 10^{54}$ ergs and $\rho_{\text{HL}}(0) = 0.2 \text{Gpc}^{-3} \text{yr}^{-1}$, the expected diffuse neutrino flux at the break energy $E_\nu^b \approx 0.05 E_p^b$ is $E_\nu^2 \Phi_\nu \sim 6 \times 10^{-11} g_{-1} \epsilon_{e,-1} \epsilon_{B,-1}^{3/2} E_{\text{ej},53} n_0^{3/2} (f_z/3) \text{GeVcm}^{-2} \text{s}^{-1} \text{sr}^{-1}$.

In the higher energies, $E_\nu^2 \Phi_\nu$ becomes larger.

In the cases where UHE nuclei can survive as demonstrated in Figs. 8 and 9, we have $f_{\text{Fe}\gamma} \lesssim 1$ at $E_{\text{Fe}} \sim 10^{20}$ eV. From Eq. (31), we obtain $f_{p\gamma} \lesssim 4 \times 10^{-3}$ at $E_p \sim 10^{20}$ eV and $f_{\text{meson,Fe}} \lesssim 0.05$. Hence, we expect the diffuse background neutrino flux, $E_\nu^2 \Phi_\nu \lesssim 10^{-9} \text{GeVcm}^{-2} \text{s}^{-1} \text{sr}^{-1}$ at $E_\nu \sim 10^{18}$ eV under the GRB-UHECR hypothesis.

VI. IMPLICATIONS TO GAMMA-RAY ASTRONOMY

Not only neutrinos but also high-energy gamma rays (originating from neutral pions, and muons, electrons and positrons from charged pions) will be produced. However, such high-energy gamma rays generally suffer from the internal attenuation processes, especially in the internal shock model, as discussed in many papers (see, e.g., [36] and references there in). The copious photon field also plays an important role on the efficient photomeson production, so that we cannot expect that GRBs are bright in $\sim \text{TeV}$ gamma rays when bright in neutrinos (see Refs. [37, 104] and references there in). In other words, when $f_{p\gamma}$ becomes small enough, we can expect that the optical depth for pair-creation $f_{\gamma\gamma}$ becomes smaller than the unity (hence high-energy gamma rays from far sources will be attenuated by CMB/CIB pho-

tons rather than seed photons in the source). As seen in the previous section, when UHE heavy nuclei can survive, $f_{p\gamma}$ is much smaller than the unity. Therefore, we may expect escape of high-energy gamma rays from the source when UHE heavy nuclei can survive. Such high-energy gamma-ray signals are useful as signatures of UHECR acceleration so that they are important, although the distinction between hadronic and leptonic components is not so easy. (When $f_{p\gamma}$ is large enough, we may not expect high-energy gamma rays due to internal attenuation. But note that proton-induced cascaded gamma-ray signals can be seen, e.g., when the baryon loading factor is large enough $\xi_{\text{acc}} \gtrsim 10$ [104, 105]. Hence, observations of high-energy gamma rays are still important as a probe of the UHECR acceleration. See also [106].)

First, let us consider the internal shock model with $\alpha = 1$ and $\beta = 2.2$. The optical depth for pair-creation process (which is usually relevant for escape of high-energy gamma rays) can be approximately written as $f_{\gamma\gamma}(\varepsilon_{\text{ob}}) \simeq 0.12\sigma_T\tilde{\varepsilon}(dn/d\varepsilon)_{\tilde{\varepsilon}}l$ [36, 107]. Here $\tilde{\varepsilon}$ is defined as $(m_e c^2)^2/\varepsilon$. When $\alpha \sim 1$, the optical depth for pair-creation $f_{\gamma\gamma}$ roughly reaches the maximum value at $\sim \tilde{\varepsilon}^b$. (Note that, in fact, $f_{\gamma\gamma}(\varepsilon)$ increases logarithmically above $\sim \varepsilon_{\text{ob}}^b$ while decreases above $\tilde{\varepsilon}_{\text{ob}}^{sa}$.) On the other hand, as seen in the previous section, $f_{N\gamma}$ is also determined by the photon field. Therefore, we can relate the two quantities. Note that, in cases of $\alpha \sim 1$, the numerically calculated $f_{N\gamma}$ by using Eq. (4) is larger than that evaluated analytically by using Eq. (5) by a factor of ~ 3 . Taking into account this factor, $f_{\gamma\gamma}$ at ε_{ob} can be written as

$$\frac{f_{\gamma\gamma}(\varepsilon_{\text{ob}})}{f_{N\gamma}(E_N)} \simeq 0.95 \left(\frac{A}{56}\right)^{-1.21} \left\{ \frac{(\varepsilon_{\text{ob}}/\tilde{\varepsilon}_{\text{ob}}^b)^{1.2}}{1} \right\} \quad (39)$$

Here, the parameter regions for the upper and lower columns are $\varepsilon_{\text{ob}} < \tilde{\varepsilon}_{\text{ob}}^b$ and $\varepsilon_{\text{ob}} \geq \tilde{\varepsilon}_{\text{ob}}^b$, respectively. From the above expressions, we can expect that the source where UHE Fe nuclei can survive ($f_{\text{Fe}\gamma} \lesssim 1$) is almost completely thin for pair-creation ($f_{\gamma\gamma} \lesssim 1$). This implies that high-energy gamma rays are expected in the prompt phase, if UHE Fe nuclei can be accelerated at internal shocks. In GRBs, acceleration of electrons (which is usually used for explanation of the prompt emission) also occurs, and very high-energy gamma rays can be produced via inverse-Compton scattering. Whether leptonic gamma rays or hadronic gamma rays are dominant, we expect that such high-energy gamma rays induce electromagnetic cascades due to the CIB/CMB when $f_{\text{Fe}\gamma} \lesssim 1$.

The above arguments can be applied to the reverse-forward shock model and hypernova model as well as the internal shock model. For example, let us consider the forward shock model. In deriving Eq. (39), let us replace ε^b , $\alpha = 1$ and $\beta = 2.2$ with ε^c , $\alpha = 1.5$ and $\beta = 2$ (for $p = 2$). As a result, the optical thickness for pair-creation at $\varepsilon_{\text{ob}} = 10^{12}$ eV can be evaluated as

$$\frac{f_{\gamma\gamma}(\varepsilon_{\text{ob}} = 10^{12} \text{ eV})}{f_{N\gamma}(E_N = 10^{20} \text{ eV})} \simeq 0.38 \left(\frac{A}{56}\right)^{-0.42} \left(\frac{\varepsilon_{\text{ob},12}}{E_{N,20}}\right)^{0.5}. \quad (40)$$

Hence, we can expect that $\sim \text{TeV}$ gamma rays escape from the source when UHE Fe nuclei can survive. Observations of the high-energy cutoff in the afterglow emission may give us clues to know whether UHE heavy nuclei, if they exist, can survive or not. However, it may be difficult to see the cutoff due to attenuation by CMB/CIB photons.

In the hypernova model, not only nonthermal photons radiated from relativistic electrons but also thermal photons (in the optical band) exist at the relatively early time. For very high-energy gamma rays to escape from the source, the optical depth against these thermal photons has to be smaller than the unity. In fact, photon spectra of hypernovae are very complicated, so that we shall make the very simple estimation by using a black-body spectrum. We have

$$f_{\gamma\gamma}(\varepsilon_{\text{ob}}) \sim 0.35 \left(\frac{kT}{1 \text{ eV}}\right) \left(\frac{r}{1 \text{ pc}}\right) \left(\frac{\varepsilon_{\text{ob}}}{1 \text{ PeV}}\right)^{-2}. \quad (41)$$

Therefore, hadronic gamma rays from high-energy neutral pions, muons and pairs above $\sim \text{PeV}$ could escape from the source. They will be cascaded by CMB/CIB photons. To predict observed spectra, we need to perform detailed numerical calculations, which is beyond scope of this paper.

As seen above, we can expect escape of high-energy gamma rays for conditions where UHE heavy nuclei can survive. They will be attenuated by CMB/CIB photons, and delayed secondary gamma rays are generated. Detection of delayed gamma-ray signals are expected only when the EGMF in the void region is weak enough (see [38] and references there in). The delayed gamma-ray flux from one GRB event depends on the delayed time due to the EGMF. The hadronic gamma-ray flux can be expressed by $f_{p\gamma}$ or f_{meson} as well as the neutrino flux. Hence, the expected diffuse gamma-ray background flux from GRBs is at most $\lesssim 10^{-8} \text{ GeV cm}^{-2} \text{ s}^{-1} \text{ sr}^{-1}$ [102]. Furthermore, we may expect cosmogenic gamma-rays as well as cosmogenic neutrinos [109]. If the EGMF in the void region is weak enough, we also expect such secondary gamma rays originating from propagating UHECRs.

VII. SUMMARY AND OUTLOOK

In this paper, we have shown that not only protons but also heavy nuclei can be accelerated up to ultra-high energies in both of HL GRBs and LL GRBs. We exploit the internal shock model, (external) reverse shock model and forward shock model. We have also discussed various implications to cosmic-ray, neutrino, gamma-ray astronomy. Especially, we study cosmic-ray acceleration in LL GRBs which may play an important role as high-energy cosmic-ray sources.

Let us summarize this paper below. First, we have shown that UHECR nuclei can be produced in both of HL GRBs and LL GRBs.

(A1) In the internal shock model, UHE protons and heavier nuclei can be produced in both of HL GRBs and LL GRBs. However, the allowed parameter range is limited. At smaller radii, most of the UHE nuclei are depleted, and a significant fraction of the nonthermal cosmic-ray energy is transferred into neutrinos. On the other hand, survival of UHE nuclei is possible only at large radii and/or for large Lorentz factors. Typically, relatively large radii $r \gtrsim 10^{15}$ cm will be required. For HL GRBs with $L_b \sim 10^{51-52}$ ergs s $^{-1}$, both of protons and heavier nuclei can be accelerated up to ultra-high energies above 10^{20} eV. For LL GRBs with $L_b \sim 10^{46-47}$ ergs s $^{-1}$, heavy nuclei can be accelerated above 10^{20} eV, while proton acceleration above such high energies may be difficult. In addition, we have shown that the effect of synchrotron self-absorption suggested by Wang et al. [17] is not so important due to the cross section in the non-resonant region.

(A2) In the (external) reverse shock model, UHE nuclei can be produced in both of HL GRBs and LL GRBs. Not only heavy nuclei but also protons achieve ultra-high energies above $\sim 10^{20}$ eV. Whether heavy nuclei can survive or not depends on various parameters, and the sufficiently low photon density is required for survival. That is, small E_{ej} , ϵ_e , ϵ_B and n are needed. Conversely, if values of these parameters are large enough, in which optical/infrared are often expected, survival of UHE nuclei is impossible. Note that UHE nuclei produced at internal shocks could be photodisintegrated by photons generated at the reverse shock, when the ejecta is in the thick ejecta regime. Hence, we could not expect survival of UHE nuclei in many cases, when we see strong optical/infrared flashes.

(A3) In the (external) forward shock model, not only heavy nuclei but also protons can achieve ultra-high energies above $\sim 10^{20}$ eV in both of HL GRBs and LL GRBs. When the photon density is sufficiently low, survival of UHE nuclei is possible. The relevant parameters $f_{N\gamma}$ and maximum energy E_N^{\max} depend on time. In the ISM case, $f_{N\gamma}$ monotonically increases with time before the jet break occurs. On the other hand, in the wind-medium case, $f_{N\gamma}$ monotonically decreases with time. We have shown that the jet-break effect can be important for survival of UHE nuclei, which was not pointed out previously. After the jet break, the photon density decreases, so that survival of UHE nuclei becomes easier.

In the internal shock model and reverse shock model, we have to assume that heavy nuclei are contained in relativistic outflows of GRBs. It is natural to consider that only light elements can be synthesized in such a highly relativistic outflows due to the high photon to baryon ratio [110, 111]. However, there may be possibility that such an outflow is contaminated with heavy nuclei that are produced by explosive nucleosynthesis [112, 113, 114, 115]. Also, such heavy nuclei can be entrained from the stellar surroundings due to Kelvin-Helmholtz instabilities and/or oblique shocks [116]. Whether entrained heavy nuclei can survive or

not is the issue that should be carefully examined. On the other hand, in the forward shock model and hypernova model, heavy nuclei will be supplied by the swept material. They could come from the stellar wind of the progenitor star, e.g., the Wolf-Rayet star.

Next, we have shown that both of HL GRBs and LL GRBs can supply the necessary energy for UHECRs as energy budgets, although there are some caveats. These two populations, if they exist, lead to very different number densities as UHECR sources. The source number density of UHECR sources will be constrained by current and future observations by PAO. In addition, if we could obtain information on the mean EGMF, we can test the GRB-UHECR hypothesis, and distinguish between the two possibilities.

(B) If the mean EGMF is strong enough $B_{EG} \lambda_{\text{Mpc}}^{1/2} \gtrsim 10^{-9}$ G Mpc $^{1/2}$ and source number density of UHECRs is not too large, HL GRBs are main UHECR candidates rather than LL GRBs, although it is difficult to exclude LL GRBs as faint UHECR-accelerator candidates. On the other hand, when the mean EGMF is weak enough $B_{EG} \lambda_{\text{Mpc}}^{1/2} \lesssim 10^{-9}$ G Mpc $^{1/2}$ and source number density of UHECRs is not too small $n_s \gtrsim 10^{-6}$ Mpc $^{-3}$, LL GRBs will be more suitable as main UHECR source candidates. It is because the weak EGMF leads to the small source number density for HL GRBs as UHECR sources. However, we have possibilities to see HL GRBs as very bright sources if HL GRBs are UHECR-accelerators. Note that, although we consider the extreme case where each population has the typical UHECR luminosity respectively, there are not necessarily clear differences between the two populations. More generally, we should take into account the distribution of the UHECR luminosity (i.e., luminosity-weighted model).

Novel results by PAO showed anisotropy of UHECR sources and suggested the correlation with AGN. However, the origin has not been revealed yet. In order to distinguish GRBs from other candidates such as AGN, it is important to find burst signatures (e.g., the existence of the critical energy and the ratio between triplets or higher multiplets and doublets). In addition, we can test whether GRBs (including HL GRBs, LL GRBs and hypernovae) become candidates of UHECR sources or not, if we obtain information on the source number density and mean EGMF. To achieve this big goal, more observations and detailed simulations are required. Future studies on small-scale and medium-scale clusterings will give us critical information on UHECR sources.

Along with the feasibility of UHECR astronomy, observations of gamma rays and neutrinos are also important. Neutrino astronomy is very useful as a direct probe of cosmic-ray acceleration, although the detection is not so easy due to weak interaction. High-energy neutrinos from GRBs have been predicted from various contexts. If we detect, we can obtain very useful information on cosmic-ray acceleration in GRBs.

(C) Cosmic-ray acceleration in GRBs can be probed by

detection of high-energy neutrinos. In fact, we can expect the detectable neutrino diffuse neutrino background in various scenarios under the GRB-UHECR hypothesis [35]. Whether UHE heavy nuclei (such as iron) can survive or not depends on various parameters, and we have shown that the neutrino detection is more difficult when we choose parameters allowing for survival of UHE heavy nuclei. Especially in the internal shock model for HL GRBs, parameters allowing for survival of UHE heavy nuclei are different from frequently used typical parameters for the prompt emission of HL GRBs. Although we could not expect survival of UHE heavy nuclei typically, survival can be still expected at sufficiently large shock radii because internal shocks can occur at various radii. Note that we can potentially constrain the averaged $f_{p\gamma}$ from current and future observations under the GRB-UHECR hypothesis. That is, neutrino observations potentially enable us to constrain the allowed parameter range under the GRB-UHECR hypothesis.

We can expect high-energy gamma-ray emissions (including leptonic and hadronic gamma rays) from GRBs as well as high-energy neutrinos. Current and future telescopes, and satellites such as GLAST, MAGIC and VERITAS may detect such high-energy gamma-ray signals, and would give us useful information on the source.

(D) Generally, high-energy gamma rays from GRBs suffer from the internal attenuation due to pair-creation, which induces electromagnetic cascades in the source. However, when UHE heavy nuclei (such as iron) can survive, high-energy gamma rays can be more expected, (although neutrino detection becomes more difficult). For the typical prompt emission spectrum, we have shown that the source is almost optically thin for pair-creation $f_{\gamma\gamma} \lesssim 1$ when $f_{\text{Fe}\gamma} \lesssim 1$. For the afterglow emission, we have also shown that $\sim\text{TeV}$ gamma rays can escape from the source when $f_{\text{Fe}\gamma} < 1$ at 10^{20} eV. Furthermore, we expect very high-energy gamma-ray emission above $\sim\text{PeV}$

in the hypernova model. Such very high-energy gamma rays will be cascaded due to the CMB/CIB and generate $\sim\text{GeV}$ delayed secondary gamma rays, which may be detected by GLAST, MAGIC and VERITAS [38]. If sources are nearby, $\sim\text{TeV}$ gamma rays may be observed by Cherenkov telescopes.

When we are preparing this work independently, we found that Wang et al. [17] studied acceleration of UHE nuclei in GRBs. In this paper, we have studied in more detail by making use of the detailed cross section and spectra of afterglows. Furthermore, we have also studied cosmic-ray acceleration in LL GRBs.

Acknowledgments

KM thanks C. Dermer because he made very profitable comments at the conference TAUP2007 on September, 2007. KM also thanks R. Blandford, S. Inoue and H. Takami. We thank R. Yamazaki and K. Toma for helpful comments. The work of KM is supported by a Grant-in-Aid for JSPS. The work of KI is supported by Grants-in-Aid for Scientific Research of the Japanese Ministry of Education, Culture, Sports, Science, and Technology 18740147 and 19047004. The work of SN is supported by Grants-in-Aid for Scientific Research of the Japanese Ministry of Education, Culture, Sports, Science, and Technology 19104006, 19740139, 19047004. The work of TN is supported by Grants-in-Aid for Scientific Research of the Japanese Ministry of Education, Culture, Sports, Science, and Technology 19047004. The work of us is supported by a Grant-in-Aid for the 21st Century Center of Excellence “Center for Diversity and University in Physics” from the Ministry of Education, Culture, Sports, Science and Technology of Japan.

-
- [1] E. Waxman, Phys. Rev. Lett., 75, 386 (1995)
 - [2] M. Milgrom and V. Usov, ApJ, 449, L37 (1995)
 - [3] M. Vietri, ApJ, 453, 883 (1995)
 - [4] T. Le and C.D. Dermer, ApJ, 661, 394 (2007)
 - [5] D. Guetta and T. Piran, JCAP, 07003 (2007)
 - [6] M.D. Kistler, H. Yuksel, J. Beacom, and K.Z. Stanek, arXiv:0709.0381
 - [7] S.D. Wick et al., Astropart. Phys., 21, 125 (2004)
 - [8] K. Murase and S. Nagataki, Phys. Rev. D, 73, 063002 (2006)
 - [9] V. Berezhinsky, A.Z. Gazizov, and S.I. Grigorieva, PRD, 74, 043005 (2006)
 - [10] R. Aloisio et al., Astropart. Phys., 27, 76 (2007)
 - [11] D. Guetta and M.D. Valle, ApJ, 657, L73 (2007)
 - [12] E. Liang et al., ApJ, 670, 565 (2007)
 - [13] D. Guetta et al., ApJ, 615, L73 (2004)
 - [14] K. Murase, K. Ioka, S. Nagataki, and T. Nakamura, ApJ, 651, L5 (2006)
 - [15] N. Gupta and B. Zhang, Astropart. Phys., 27, 386 (2007)
 - [16] X.Y. Wang, S. Razzaque, P. Mészáros, and Z.G. Dai, Phys. Rev. D, 76, 083009 (2007)
 - [17] X.Y. Wang et al., arXiv:0711.2065
 - [18] K. Greisen, Phys. Rev. Lett. 16, 748 (1966)
 - [19] G.T. Zatsepin and V.A. Kuz'min, Sov. Phys. JETP. Lett., 4, 78 (1966)
 - [20] Pierre Auger Collaboration, Science, 318, 938 (2007)
 - [21] Pierre Auger Collaboration, arXiv:0712.2843
 - [22] C.D. Dermer, arXiv:0711.2804 (2007)
 - [23] Pierre Auger Collaboration, arXiv:0706.1495
 - [24] D. Gorbunov et al., arXiv:0711.4060
 - [25] T. Wibig and A.W. Wolfendale, arXiv:0712.3403
 - [26] J. Ahrens et al., Astropart. Phys., 20, 507 (2004)
 - [27] U.F. Katz, Nucl. Instrum. Meth., A567, 457 (2006)
 - [28] S.W. Barwick et al., Phys. Rev. Lett., 96, 171101 (2006)
 - [29] V. Van Elewyck et al., astro-ph/0612731 (2006)
 - [30] E. Waxman and J. Bahcall, Phys. Rev. Lett., 78, 2292 (1997)

- [31] E. Waxman and J. Bahcall, *ApJ*, 541, 707 (2000)
- [32] Z.G. Dai and T. Lu, *ApJ*, 551, 249 (2001)
- [33] C.D. Dermer, *ApJ*, 574, 65 (2002)
- [34] K. Murase and S. Nagataki, *Phys. Rev. Lett.*, 97, 051101 (2006)
- [35] K. Murase, *Phys. Rev. D*, 76, 123001 (2007)
- [36] K. Murase and K. Ioka, *arXiv:0708.1370*
- [37] C.D. Dermer, E. Ramirez-Ruiz, and T. Le, *ApJ*, 664, L67 (2007)
- [38] K. Murase, K. Asano, and S. Nagataki, *ApJ*, 671, 1886 (2007)
- [39] T. Piran, *Rev. Mod. Phys.*, 76, 1143 (2005)
- [40] P. Mészáros, *Rep. Prog. Phys.*, 69, 2259 (2006)
- [41] B. Zhang, *Chin. J. Astron. Astrophys.*, 7, 1 (2007)
- [42] R. Blandford and D. Eichler, *Phys. Rep.*, 154, 1 (1987)
- [43] Note that expressions of $dn_{CR}/d\varepsilon_{CR}$ and $n_{\varepsilon, \max}$ in Ref. [35] included trivial typos. The expressions given in this paper is correct. Of course, all the results in Ref. [35] were calculated using the correct expressions.
- [44] U. Keshet and E. Waxman, *Phys. Rev. Lett.*, 94, 111102 (2005)
- [45] M. Vietri, *ApJ*, 591, 954 (2003)
- [46] J. Aoi, K. Murase, and S. Nagataki, *MNRAS*, 383, 1431 (1998)
- [47] J.P. Rachen and P. Mészáros, *Phys. Rev. D*, 58, 123005 (1998)
- [48] Y.A. Gallant and A. Achterberg, *MNRAS*, 305, L6 (1999)
- [49] A. Achterberg, Y.A. Gallant, J.G. Kirk, and A.W. Guthmann, *MNRAS*, 328, 393 (2001)
- [50] C.D. Dermer, *ApJ*, 664, 384 (2007)
- [51] F.W. Stecker and M.H. Salamon, *ApJ*, 512, 521 (1999)
- [52] S. Agostinelli et al., *Nuclear Instruments and Methods in Physics Research A*, 506, 250-303 (2003), <http://wwwasd.web.cern.ch/wwwasd/geant4/geant4.html>
- [53] Particle Data Group, <http://pdg.lbl.gov/>
- [54] J.L. Puget, F.W. Stecker, and J.H. Bredekamp, *ApJ*, 205, 638 (1976)
- [55] S. Karakula and W. Tkaczyk, *Astropart. Phys.*, 1, 229 (1993)
- [56] D. Allard et al., *A&A*, 443, L29 (2005)
- [57] K. Asano, *ApJ*, 623, 967 (2005)
- [58] K. Ioka, K. Murase, K. Toma, S. Nagataki, and T. Nakamura, *ApJ*, 670, L77 (2007)
- [59] S. Campana et al., *Nature*, 442, 1008
- [60] E. Waxman et al., *ApJ*, 667, 351 (2007)
- [61] X.Y. Wang et al., *ApJ*, 664, 1026 (2007)
- [62] Y.Z. Fan, T. Piran, and D. Xu, *JCAP*, 09013 (2006)
- [63] G. Ghisellini, G. Ghirlanda, and F. Tavecchio, *MNRAS*, 375, L36 (2007)
- [64] K. Toma et al., *ApJ*, 659, 1420 (2007)
- [65] D. Malesani et al., *ApJ*, 609, L5 (2004)
- [66] P.W.A. Roming et al., *ApJ*, 652, 1416 (2006)
- [67] F. Genet, F. Daigne, and R. Mochkovitch, *MNRAS*, 381, 732 (2007)
- [68] L.Z. Uhm and A.M. Beloborodov, *ApJ*, 665, L93 (2007)
- [69] D. Eichler and E. Waxman, *ApJ*, 627, 861, (2005)
- [70] K. Toma et al., *arXiv:0709.3332*
- [71] A.R. Bell, *MNRAS*, 353, 550 (2004)
- [72] M. Milosavljević and E. Nakar, *ApJ*, 641, 978 (2006)
- [73] C.D. Dermer and M. Humi, *ApJ*, 556, 479 (2001)
- [74] R. Wijers and T. Galama, *ApJ*, 523, 177 (1999)
- [75] S.T. Scully and F.W. Stecker, *Astropart. Phys.*, 16, 271 (2002)
- [76] V. Berezhinsky, A.Z. Gazizov, and S.I. Grigorieva, *hep-ph:0204357* (2002)
- [77] M. Vietri, D.D. Marco, and D. Guetta, *ApJ*, 592, 378 (2003)
- [78] E. Waxman, *ApJ*, 606, 988 (2004)
- [79] T. Yamamoto, for the Pierre Auger Collaboration, *arXiv:0707.2638*
- [80] D. Kocevski and N. Butler, *arXiv:0707.4478*
- [81] A.M. Soderberg et al., *ApJ*, 638, 930 (2006)
- [82] More precisely, in order to evaluate the total radiation energy rate, we have to take into account that the detection flux threshold is different among detectors.
- [83] K. Ioka et al., *A&A*, 458, 7 (2006)
- [84] Achterberg et al., *ApJ*, 664, 397 (2007)
- [85] Achterberg et al., *arXiv:0705.1186*
- [86] P.P. Kronberg, *Rep. Prog. Phys.*, 57, 325 (1994)
- [87] J.P. Vallée, *New Astron. rev.*, 48, 763 (2004)
- [88] K. Dolag et al., *JCAP* 01009 (2005)
- [89] H. Takami and K. Sato, *ApJ*, 639, 803 (2006)
- [90] H. Takami and K. Sato, *arXiv:0711.2386*
- [91] J. Miralda-Escudé and E. Waxman, *ApJ*, 462, L59 (1996)
- [92] E. Waxman and J. Miralda-Escudé, *ApJ*, 472, L89 (1996)
- [93] D. Harari, S. Mollerach, and E. Roulet, *JCAP*, 11012 (2006)
- [94] S.L. Dubovsky, P.G. Tinyakov, and I.I. Tkachev, *Phys. Rev. Lett.*, 85, 1154 (2000)
- [95] D. Harari, S. Mollerach, and E. Roulet, *JCAP*, 05010 (2004)
- [96] M. Kachelriess and D. Semikoz, *Astropart. Phys.*, 23, 486 (2005)
- [97] H. Takami and K. Sato, *arXiv:0710.1434*
- [98] L. A. Anchordoqui et al., *Astropart. Phys.*, in press (2007)
- [99] H. Yuksel and M.D. Kistler, *Phys. Rev. D*, 75, 083004 (2007)
- [100] H. Takami, K. Murase, S. Nagataki, and K. Sato, *arXiv:0704.9709*
- [101] D. Allard et al., *JCAP*, 09005 (2006)
- [102] E. Waxman and J. Bahcall, *Phys. Rev. D*, 59, 023002 (1998)
- [103] D. Guetta, M. Spada, and E. Waxman, *ApJ*, 559, 101 (2001)
- [104] C.D. Dermer and A. Atoyan, *New. J. Phys.* 8, 122 (2006)
- [105] K. Asano and S. Inoue, *ApJ*, 671, 645 (2007)
- [106] Too large baryon loading factors can change a seed photon spectrum below $\sim \text{GeV}$ significantly, which may seem implausible. Hence, the baryon loading factor could be constrained from observations of high-energy gamma rays. However, note that the amount of hadronic gamma rays largely depends on $f_{p\gamma}$ when $f_{p\gamma} \lesssim 1$. This implies that the flux of proton-induced gamma rays is rather sensitive to the lower photon index α . Although there were some theoretical calculations [104, 105], the lower photon index is $\alpha \sim 1.5$ expected in fast cooling synchrotron spectra, rather than the typical value $\alpha \sim 1$. It can lead to the overestimation of hadronic gamma rays.
- [107] R. Svensson, *MNRAS*, 227, 403 (1987)
- [108] Note that typical parameters for afterglows allow for high-energy TeV emissions. In fact, many predictions of TeV emissions have been done by various authors.
- [109] E. Waxman and P. Coppi, *ApJ*, 464, L75 (1996)
- [110] J. Pruet, S. Guiles, and G.M. Fuller, *ApJ*, 580, 368

- (2002)
- [111] M. Lemoine, *A&A*, 390, L31 (2002)
 - [112] S. Nagataki, A. Mizuta, S. Yamada, H. Takabe, and K. Sato, *ApJ*, 596, 401 (2003)
 - [113] K. Maeda, K. Nomoto, *ApJ*, 598, 1163 (2003)
 - [114] S. Nagataki, A. Mizuta, and K. Sato, *ApJ*, 647, 1255 (2006)
 - [115] N. Tominaga, *arXiv:0711.4815*
 - [116] W.Q. Zhang, S.E. Woosley, and S.E. MacFadyen, *ApJ*, 586, 356 (2003)